Interannual variations of Arctic cloud types in relation to sea ice

Ryan Eastman

A thesis

submitted in partial fulfillment of the

requirements for the degree of

Master of Science

University of Washington

2009

Program Authorized to Offer Degree:

Department of Atmospheric Sciences

University of Washington

Graduate School

This is to certify that I have examined this copy of a master's thesis by

Ryan Eastman

and have found that it is complete and satisfactory in all respects,

and that any and all revisions required by the final

examining committee have been made.

Committee Members:

_____

Stephen Warren

_____

Cecilia Bitz

_____

Robert Wood

Date:_____

University of Washington

Abstract

Interannual variations of Arctic cloud types in relation to sea ice

Ryan Eastman

Chair of the Supervisory Committee:
Professor Stephen Warren
Department of Atmospheric Sciences

Interannual variations in sea ice extent and thickness may be affected by cloud radiative effect (CRE), and sea-ice changes may in turn impart changes to cloud cover. Visual cloud reports from land and ocean regions of the Arctic are analyzed for total cloud cover and 9 cloud types.

Over the high Arctic, cloud cover shows a distinct seasonal cycle dominated by low stratiform clouds which are much more common in summer than winter. Year to year variations of cloud amounts over the Arctic Ocean show significant correlations with surface air temperature, total sea ice extent, and the Arctic Oscillation. Low September ice extent is generally preceded by a summer with decreased middle and precipitating clouds. Following a low-ice September there is enhanced cumulonimbus and stratus in autumn. Total cloud cover appears to be greater throughout the year during low ice years.

The multidecadal trends from surface observations over the Arctic Ocean show increasing cloud cover, which may promote ice loss by the longwave effect. The trends are positive in all seasons, but most significant during spring

and autumn, when cloud cover is positively correlated with surface temperature. The coverage of summertime precipitating clouds has been increasing over many Arctic land areas but decreasing over all parts of the Arctic Ocean; this oceanic trend may promote ice loss.

Trends in surface cloud data over the Arctic as a whole disagree with those from AVHRR and TOVS satellite data, especially in autumn and winter. At smaller geographic scales, time series of surface and satellite observed cloud cover show some agreement except over ice during winter.

TABLE OF CONTENTS

LIST OF FIGURES

Figure Number Page

LIST OF TABLES

Table Number Page

ACKNOWLEDGEMENTS

An advance version of the ocean cloud update was provided by Carole Hahn. Axel Schweiger provided TOVS data, and Jeff Key and Xuanji Wang provided updated APP-x data. We thank J. Michael Wallace, Cecilia Bitz, Robert Wood, and Axel Schweiger for helpful discussion. The research was supported by NSF's Climate Dynamics Program and NOAA's Climate Change Data and Detection (CCDD) program, under NSF Grants ATM-06-30428 and ATM-06-30396.

1. INTRODUCTION

Arctic climate has changed dramatically in the past two decades. The end-of-summer ice extent has declined, and reached surprisingly small values in 2007 and 2008 (Stroeve 2008; NSIDC 2008). This shrinking ice cover has been accompanied by an increase in surface air temperature of almost 0.5˚C per decade from 1979 through 2003 as observed by the International Arctic Buoy Programme (Rigor et al. 2000).

Clouds are thought to have an important role in the Arctic climate system, though the exact nature of their role is not completely understood, and the climate modeling studies done have not been well substantiated by observations. Vavrus (2004) modeled arctic greenhouse warming including cloud feedbacks, concluding that ~40% of the Arctic warming was due to cloud changes resulting from the warming. Beesley (2000) modeled the seasonal cycle of ice thickness, finding that an increase of low clouds would lead to thicker ice, and an increase of high clouds would lead to thinner ice. Francis and Hunter (2006) analyzed infrared sounding data from satellites, and found a positive correlation between ice extent and downward longwave cloud radiative effect, suggesting that the longwave radiation emitted by clouds can cause sea-ice melt. Francis and Hunter also stated that cloud phase may be related to the anomalies of downward longwave radiation, with water clouds emitting more

longwave radiation than ice clouds because they are optically thicker and therefore have higher emissivity. Shupe and Intrieri (2004) agree, stating that cloud phase, temperature and height (which are all related) have a strong impact on CRE. Their research, which was part of the 'Surface Heat Budget of the Arctic' (SHEBA) program and employed radar, lidar, pyranometer, radiometer, and radiosonde data from 1997 and 1998, indicates that for longwave radiation, the majority of radiatively significant cloud scenes have bases lower than 4.3 km and cloud temperatures greater than -31˚ C.

Cloud radiative over the Arctic likely has a significant seasonal dependence. Most studies agree that clouds have a warming effect during all seasons except summer. The warming is due to the emission of longwave radiation by clouds, while the cooling effect in summer is due to scattering of incoming shortwave radiation. The longwave warming dominates throughout the dark months in the Arctic, while the shortwave cooling can only take place during the summer when the sun is high and the snow has melted so that the surface albedo is lower. The exact timing and duration of the negative CRE is not agreed upon. Again using SHEBA data, Intrieri et al. (2002) found only a few weeks during mid-summer when CRE is negative. Using a 1D coupled model, Curry and Ebert (1992) also determined that CRE over the Arctic is positive except for two weeks during midsummer. Walsh and Chapman (1998) used radiation measurements taken on drifting Russian weather stations as well

as NCEP and ECMWF reanalysis data and inferred negative CRE from May through July. The net CRE was near zero in April and August and positive from September through March. Using the GENESIS2 general circulation model (GCM), which was claimed to compute Arctic cloudiness particularly well, Vavrus (2004) showed negative CRE only from June through August. Values and durations of positive and negative CRE most likely vary based on latitude and on the time of melt onset, which alters the surface albedo and which changes from year to year. Kay et al. (2008) postulate that a lack of summertime cloudiness in the western Arctic contributed to the dramatic ice loss of 2007. To summarize the previous work, it seems safe to assume that clouds generally warm the arctic surface through longwave radiative more than they cool the surface by reflecting sunlight, except during the summer months.

The interaction of clouds with surface conditions goes both ways: Surface changes can also impart changes upon cloud cover. Schweiger et al. (2008) used 40 year ECMWF Re-Analysis (ERA-40) data as well as TIROS Operational Vertical Sounder Polar Pathfinder (TOVS Path P) and determined that sea ice retreat during autumn is linked to a decrease in low clouds, with low-cloud cover increasing in altitude near ice margins due to an increase in surface temperature and a subsequent decrease in static stability. Whether cloud changes are responsible for arctic sea ice and temperature changes, or vice-versa, has to do with the seasonality of the changes.

Published studies of Arctic cloud trends show little consistency with one another. Wang and Key (2005) used Advance Very High Resolution Radiometer (AVHRR) satellite data from 1982 to 1999, obtaining trends of -6, +3, +2, and -2 percent per decade during winter, spring, summer and autumn respectively. These trends are for the entire area north of 60° N, and the seasons are December, January, February (DJF); March, April, May (MAM); June, July, August (JJA); and September, October, November (SON) respectively. Schweiger (2004) used satellite data from the TOVS Path P between 1980 to 2001 for all ocean areas north of 60° N, finding seasonal trends of -4, +5, +0 and +0 percent per decade, for winter through autumn respectively. Using surface weather observations from 1971 to 1996, Warren, Eastman and Hahn (2007, figure 7) found large positive cloud cover trends over the Arctic land area in winter and spring, and small negative trends in summer and autumn. These three studies disagree in many places, but also represent differing regions and time spans (We will see below that when another 11 years are added to the surface data set the trends are positive in all seasons) though they do all agree upon the presence of a positive trend in cloud cover during springtime. Retrieval of cloud properties from satellites over ice is often difficult, because clouds offer little contrast from the surface in albedo or temperature. Pixel size is a concern, considering that many pixels are only partially filled with clouds, so small-scale structures of clouds indicative of cloud type are not detectable. A

pixel may also contain a mixture of sea ice and open water. Also, the satellite data begin around 1980, limiting the period of record for analysis of interannual variations and trends. The intercomparison of these three data sets will be examined in more detail in section 6 below.

General circulation models have been predicting changes in Arctic clouds and precipitation in response to global warming from greenhouse gases. Vavrus (2004), using GENESIS2 under 2 x CO_2 , predicts an increase in low-level cloud cover and an increase of 19% in Arctic precipitation after a roughly 20 year equilibration period. Using the CCSM3 model; Vavrus et al. (2008a) also predict an increase in future Arctic cloudiness, especially in autumn and winter. The increase in the CCSM3 cloud cover is due to increased evaporation from a warmer Arctic ocean. Also using the CCSM3, Gorodetskaya and Tremblay (2008) predict an increase in cloud liquid water path (LWP), especially in winter. This increase in cloud liquid water brings about increasing positive longwave CRE. Using a model ensemble mean, Vavrus et al. (2008b) predict a cloudier Arctic, especially during autumn and at low and high levels. Little change is predicted at the middle level, and a decrease is predicted very near the surface (fog). The predicted decrease in fog may be related to the processes described by Schweiger et al. (2008), with ice retreat exposing more open water and thus reducing static stability. Walsh et al. (2002) also used an ensemble of numerous GCM's and found a consistent model projection for increased

precipitation, though these models are shown to substantially overpredict the amount of currently observed precipitation. On the other hand, Warren et al's. (1999) analysis of drifting-station measurements found a decrease of May snow depth on multi-year sea ice from 1954 to 1991, suggesting that its cause was a decrease in wintertime snowfall. A consensus among modeling studies is that an increase in both precipitation and clouds is expected as the arctic warms, especially low and liquid clouds, but with the exception of fog. The predicted changes in low clouds and cloud LWP suggest that there will be an increase in downwelling longwave radiation, furthering arctic warming during non-summer months.

The Arctic Ocean exhibits a dramatic seasonal cycle of cloud cover, which models have attempted to explain. Vowinckel (1962) showed wintertime cloud (from drifting-station reports) cover steady at a low value, jumping up to a higher summer value in May and dropping just as abruptly in September-October. The pattern was more pronounced at higher latitudes. His plot was reproduced by Vowinckel and Orvig (1970), and the pattern for 80-90° N was confirmed in more recent surface observations by Hahn et al. (1995, Figure 13a). Wang and Key (2005, Figure 2) compared Arctic cloud climatologies from surface observations, TOVS Path P, and AVHRR satellite data for areas north of 80° N. All three agree that there is a summertime maximum in Arctic cloud cover and a minimum in April. Using SHEBA lidar and radar, Intrieri et al.

(2002) showed that cloud cover occurred most frequently in September and least frequently during February. The SHEBA data also showed that cloud phase varied seasonally, with mainly liquid clouds in summer (95% liquid clouds in July) and mostly ice clouds in winter (25% liquid clouds in December). Walsh et al. (1998) compared numerous precipitation studies and models for areas north of 70° N. The comparison indicated that precipitation has a summertime maximum, following the cloud cycle, and that precipitation amounts were lower at higher latitudes. Walsh et al. also showed that GCM's typically overestimate precipitation amounts, though the models do grasp the yearly cycle of precipitation well. The consensus of observational studies and models is that the Arctic experiences a seasonal cycle in cloud cover and precipitation, with peaks of precipitation, cloud cover and cloud liquid water content (LWC) during summertime and a minimum in cloud cover and precipitation in late winter/early spring, while the LWC minimum occurs earlier in winter around December.

Arctic climate variations and changes can be tied to changes in circulation, such as the Arctic Oscillation (AO). In its positive phase, the AO is characterized by an increase in mid-latitude westerlies, decreased sea level pressure over the Arctic and altered large-scale wind patterns over the Arctic. Since 1989 the AO index has been more positive than in the past. Rigor et al. (2002) showed that a high wintertime AO brings about low ice concentration in

the East Siberian and Laptev Seas. This occurs because the Beaufort Gyre slows during high AO years, and this reduction causes a decline in ice recirculation. According to Rigor et al. (2002), the AO can explain 64% of the variance in eastern Arctic sea-ice concentration. An Arctic cloud response to the AO has not been investigated, but could be important in enhancing or reducing the effects of the AO on sea ice concentration and Arctic temperature.

This work will further investigate seasonal cycles and interannual variations of all cloud types over Arctic land and ocean areas from 1954 to 2007, and their relations to surface temperature, ice extent, and the Arctic Oscillation.

2. DATA

Cloud data for this study come exclusively from surface synoptic observations reported from weather stations on land, from drifting stations on sea ice, and from ships. The observations are reported in the synoptic code of the World Meteorological Organization (WMO, 1974). The reports were processed into a database of individual cloud reports known as the Extended Edited Cloud Reports Archive (EECRA, Hahn and Warren, 1999; 2009). The EECRA data were averaged over monthly and seasonal time periods to create a surface-observation-based cloud climatology (Hahn and Warren 2003; 2007) for each weather station on land and for grid boxes of 5x5-degree latitude/longitude resolution over land and 10x10-degree resolution over the ocean. The grid boxes are equal-area boxes, meaning that the longitude bounds increase toward the pole. For this work, a regional climatology has been created for the Arctic, which is defined as all area over land and ocean north of 60° N.

Surface observations are generally reported eight times daily, at 00:00 UTC and at three-hour intervals thereafter. Cloud amounts are reported in octas (eighths), with sky cover (N) ranging from 0 to 8. A "sky obscured" value (N = 9) can also be reported. Sky-obscured observations are further processed using the present-weather code, to determine the cause of the obscuration

(usually fog or precipitation) and assigning a corresponding cloud type if appropriate. Cloud types are reported at three levels: low, middle and high. Middle and high observations are fewer in number because upper levels are often obscured by lower clouds. In two-layer situations, a random-overlap assumption is made to determine the amount of upper level cloud from the reports of N and the low cloud amount (Nh). When the middle and/or upper level cannot be seen because of lower overcast, no information is available. For these situations, the average frequency and amount-when-present are assumed to be the same as when those levels can be seen.

The cloud observations from land stations have been processed for the period 1971-2007. Original data come from the Fleet Numerical Oceanography Center (FNOC) from 1971 to 1976, the NCEP archive from 1977 to 1996, and the Integrated Surface Database (ISD) archive from 1997 through 2007, which is available through the National Climatic Data Center (NCDC, DSI 3505). A total of 638 individual synoptic stations in the Arctic are used in this study; they were selected for having long periods of record. The station distribution is shown in Figure 1.

Also contained in the EECRA are ship reports. Observations over ocean areas have been recorded by surface observers on ships, and in the case of the Arctic Ocean, Russian weather stations drifting on sea ice. The ocean cloud observations have been processed for 1954-2008 and entered into the EECRA

(2009 update of Hahn and Warren, 1999). The original data source was the 'Comprehensive Ocean-Atmosphere Data Set' (COADS, Woodruff et al., 1987, 1998; Worley et al. 2005). For our climatology, ocean cloud observations are organized into grid-box average values for long-term means and yearly means for months and seasons. The grid boxes used are shown by the dotted lines in Figure 1. The cloud-cover value we report for a box is the mean of all observations (land and ocean separated) taken within the box over a specified time period. Figure 2 shows the average number of cloud observations (in hundreds) per year within each grid box.

The EECRA contains individual reports with variables for total cloud cover, cloud amount at low, middle and high levels, cloud type at three levels, base height for the lowest cloud level, non-overlapped cloud amount for middle and high clouds, and a present weather code. Meteorological variables such as pressure, temperature, wind and humidity are also included in the EECRA.

The archive has non-cloud variables such as solar altitude and relative lunar illuminance that are used to calculate the sky brightness indicator, which dictates whether sufficient light was present to make a reliable cloud observation at night. Hahn et al. (1995) developed a criterion for adequate illuminance; it corresponds to the brightness of a half moon at zenith or a full moon at 6° elevation. This requirement allows the use of ~38% of the observations made with the sun below the horizon.

Weather stations were selected for use in the cloud climatology according to criteria given by Warren et al. (2007): 1) The stations normally report cloud types. 2) The stations have sufficiently long records for trend analysis. Specifically, a station must have 20 observations per month in January or July for a minimum of 15 years. 3) Stations must have an adequate number of day and night observations; in this case 15% or more of total observations must be taken at night. Since in the Arctic the solar illumination varies more with the seasonal cycle than with the day-night cycle, the climatology in this study uses a day-night average value for cloud amounts, where day is defined as all observations taken between 0600 and 1800 local time.

We develop a climatology of total cloud cover and the amounts of nine cloud types: five low cloud types (cumulonimbus (Cb), cumulus (Cu), stratus (St, stratocumulus (Sc), and fog), three middle cloud types (altocumulus (Ac), altostratus (As), and nimbostratus (Ns)), and one type for high (cirriform) clouds. For some parts of this study we add the amounts of two or more types in a group: low clouds, middle clouds, precipitating clouds (Ns, Cb), and non-precipitating middle clouds (Ac, As).

Methods used to compute average cloud amounts for the climatology are described by Warren and Hahn (2002) and on the website www.atmos.washington.edu/CloudMap. Time-averaged amounts, frequencies, and amounts-when-present are made for seasonal and monthly means every

year, as well as long-term-averaged seasonal and monthly means for the entire period of record.

In order to study the entire Arctic as a whole, or large sub-regions within the Arctic, and to gain improved statistical significance, composite time series have been created by grouping together data from many land stations and/or ocean grid boxes. The methods of averaging cloud data over large areas are designed to reduce possible biases. For example, a grid box on land may contain several stations with different climates, and the number of active stations may change during the span of years studied. Therefore, over land areas the cloud amount at a station is first converted to the anomaly of cloud amount by subtracting the long-term-station-mean cloud amount from individual yearly values. These yearly anomalies are then averaged within an equal-area grid box, weighted by number of observations at each station. Since cloud amounts in ocean grid boxes are already averaged throughout the grid box, only yearly anomalies in cloud amount have to be calculated. After this point, land or ocean grid boxes are treated in the same way when averaged over a larger area.

When we examine solely land or ocean within the larger area, yearly values of anomalies within the grid boxes are averaged together, weighted by the area of land or ocean within each box. When we examine a region containing both land and ocean, anomaly time series are calculated separately

for land and ocean for the entire region, then the yearly values are averaged, weighted by the relative area of land and ocean within the larger region. This produces one time series of percent cloud anomaly with as little bias as possible.

When studying composite regions within the Arctic Ocean, coastal and island stations are used and treated identically to ship observations. This required weighting all yearly anomalies from coast/island stations within a grid box as well as yearly anomalies from ship/drifting station observations within the box by the number of observations and then computing the yearly anomaly of the box mean. The regional mean anomaly was then computed by weighting the individual grid-box anomalies by the area of the Arctic Ocean within that box. In this way it was possible to use observations from coastal and island stations as well as ships and drifting stations to study interannual variations in clouds over the Arctic Ocean.

Trends in composited data are considered significant if their magnitude exceeds their standard deviation. Ocean-only composites span from 1954 through 2008. Composites of land and ocean combined, as well as the Arctic Ocean composite time series, span from 1971 through 2007.

For work comparing the surface observed cloud climatology to other data, we chose two satellite-derived cloud cover time series which have long periods of record over the Arctic. Both datasets only report percent cloud cover with no cloud type or height information, so only total cloud cover is compared.

The first dataset is the AVHRR Polar Pathfinder (APP-x) data by Wang and Key (2005), spanning the period 1982 - 2004 on the 25-km EASE grid (Brodzik & Knowles 2002). APP-x averages covering all land and ocean area north of 60° N were used for this project. Data updated through 2004 were provided in a personal communication from Wang and Key. The second satellite data set is the TOVS Path P data spanning 1980 - 2005 (Francis & Schweiger 1999, 2008). The TOVS has primarily been used by Schweiger (2004) over ocean areas only, though for the purpose of this comparison, a patch of land is also studied. TOVS data are organized on the EASE 100-km grid, and for this study, ocean areas are required to be composed of grid boxes made up of 100% ocean cover based on AVHRR global land cover data on the 1 km EASE grid (Knowles 2004).

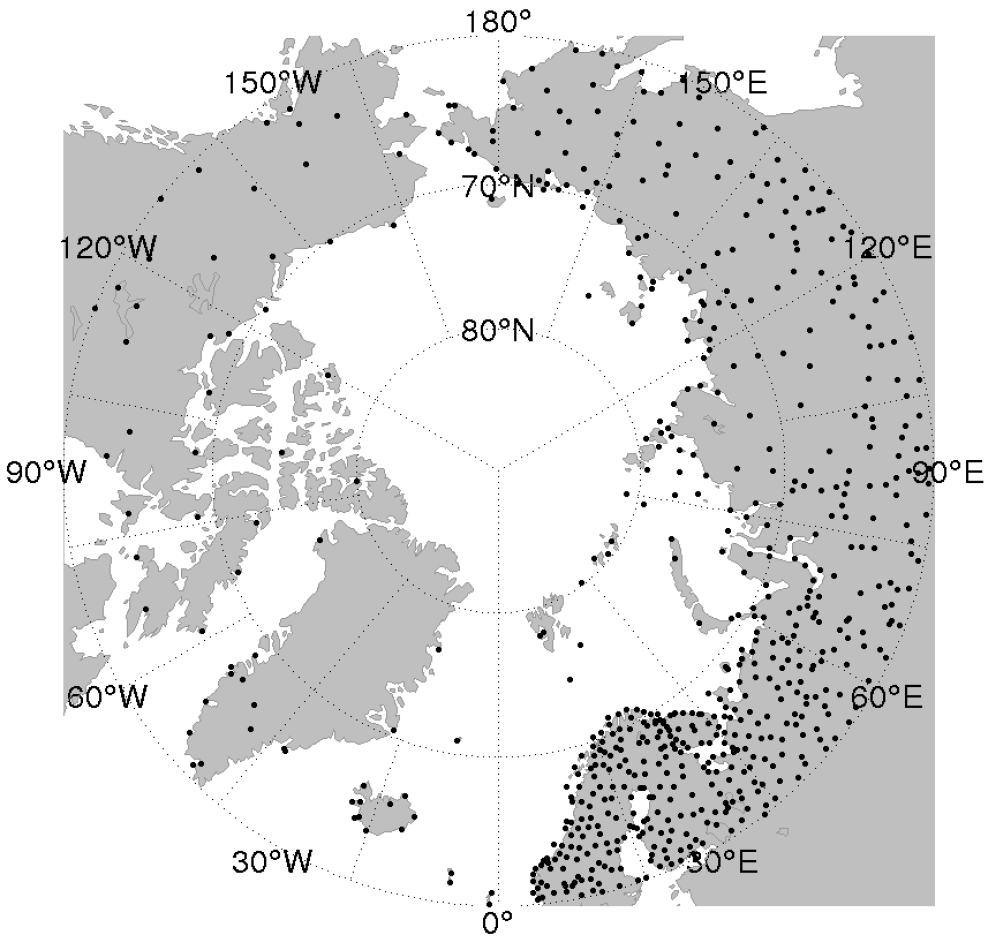

Figure 1, Distribution of Weather Stations. Surface weather stations used in this study.

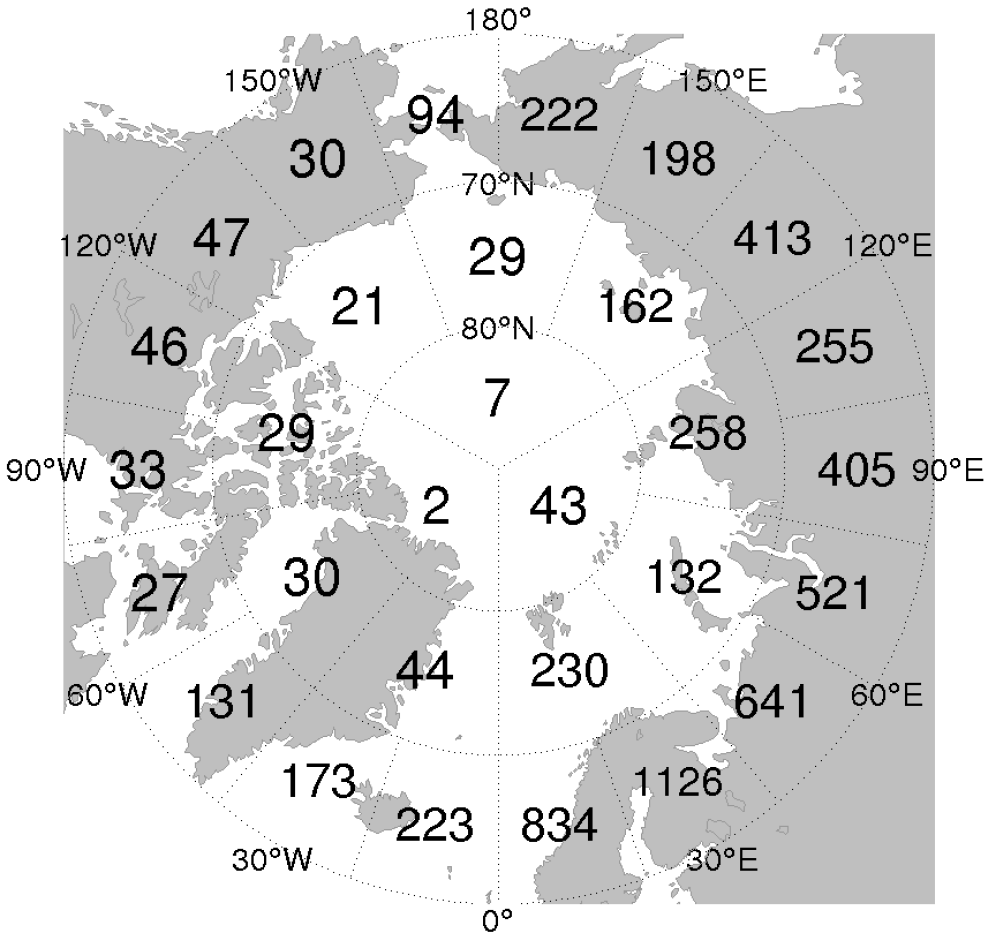

Figure 2, Number of Observations per Year. Average number of observations per year (hundreds).

3. ARCTIC CLOUD AMOUNTS AND THE SEASONAL CYCLE

Average cloud amounts are determined for total cloud cover and nine cloud types for the grid boxes shown in Figure 2, whose dimensions are approximately 500 km on a side. Grouping of boxes is done in order to reduce statistical noise and to observe geographical patterns in cloud cover for this analysis. We group boxes by latitude, or by the similarity of their cloud climatologies (particularly their seasonal cycles). Long-term mean cloud amounts, from which anomalies are computed below, cover the span 1971 to 1996 over land and 1954 to 1997 over the ocean. These long-term means are the values archived as NDP-026D and NDP-026E (Hahn and Warren 2003; 2007; www.atmos.washington.edu/CloudMap).

Mean cloud amounts over land and ocean areas in the Arctic are shown for each type and each season in Table 1. Ocean areas are cloudier than land areas at low levels and less cloudy at higher levels. The dominant cloud types are Sc, Ns, Ac and high clouds. Clear-sky scenes are not common in the Arctic, but are more frequent over land than over the ocean.

A strong seasonal cycle is present in Arctic cloud cover, with summer cloudier than winter. Figure 3a shows that the cycle is more pronounced at higher latitude. This figure closely resembles a similar figure presented by Vowinckel (1962) and Vowinckel and Orvig (1970), but our values are higher in

winter, consistent with Hahn et als finding of a positive multidecadal trend in wintertime cloud cover from 1954 to 1991. Figure 3b shows that this cycle is primarily attributable to low stratiform cloud cover, the sum of the three types St, Sc, and fog. These low types show a dramatic rise from April to May and a slower decline in autumn.

The aforementioned cycle, when studied more carefully, shows a less direct relationship with latitude and instead becomes more geographically dependent upon land masses and oceanic regions in the Arctic. For the next few figures we divide the Arctic land and ocean regions each into two separate climatic regions, "High Arctic" and "Low Arctic", based on their seasonal cycles of total cloud cover (Figure 4). The "High Arctic" regions are characterized by the sharp rise in total cloud cover during spring and subsequent sharp decline during autumn. The criterion for defining the High Arctic is a rise of at least 5% in total cloud cover between April and May and a drop of at least 5% between October and November. A high arctic regime over the ocean is required to have 10% more cloud cover during the cloudy season than in the non-cloudy season. Over land, a high arctic regime only has to have greater cloud cover between April and October than the rest of the year. The distinct rise and fall of the high arctic pattern is not present in the Low Arctic, where the seasonal cycle is much weaker. The boundary separating High Arctic from Low Arctic is different for land than for ocean (Figure 4).

The seasonal pattern of cloud cover over the High Arctic on both land and ocean (Figure 5) is shown to be almost entirely caused by the seasonal cycle of low stratiform cloudiness, which again is the sum of St + Sc + fog. The individual cycles for these three types, as well as for nimbostratus (Ns), are shown in Figure 6. Nimbostratus was excluded from the sum in Figures 3 and 5 because the atmospheric conditions associated with it are different than for the other stratiform types. A midsummer increase in fog compensates for decreases in St and Sc, resulting in a nearly constant value of St + Sc + fog through the summer.

The springtime increase of stratus clouds over the Arctic Ocean was attributed by Herman and Goody (1976) to northward advection of water vapor from the warming waterlogged tundra surrounding the ocean. Using aircraft and ECMWF analysis data, Curry and Herman (1985) claimed that the large low-cloud amount observed in June of 1980 over the Beaufort Sea was due to low level moisture advection and cooling due to radiation and boundary-layer turbulence. That interpretation was challenged by Beesley and Moritz (1999), who instead attributed the seasonal cycle of low stratiform clouds to the presence of ice crystals in winter clouds and their absence in summer clouds. Their model showed that below a threshold temperature of -10 to -15° C, the residence time of cloud particles decreased substantially, reducing the time-average cloud cover.

Figure 7 shows the seasonal cycles of the remaining cloud types. For the middle and high clouds, the cloud-type amounts shown include our estimates of the amounts hidden above lower clouds, using the random-overlap assumption (Hahn and Warren, 1999). Because of overlap, the sum of the individual cloud-type amounts exceeds the total cloud cover.

Altocumulus Ac exhibits an increase in summer, smaller and less abrupt than that of low stratiform clouds. The seasonal cycle of high (cirriform) clouds is nearly a mirror-image of that of Ac, and As shows no seasonal cycle, so that the sum of Ac, As, and high clouds is nearly constant through the year. Cumulonimbus exhibits opposing seasonal cycles in the High Arctic and Low Arctic regions. The High Arctic Ocean has almost no Cb at any time. The Low Arctic land has Cb in summer but not in winter, but the Low Arctic ocean has a much higher Cb amount in winter. This winter maximum is most likely due to the prevalence of cold-air outbreaks over open water in the Low Arctic region, triggering open cellular convection or cloud streets. This situation occurs frequently in areas of warm ocean downwind of cold land, particularly the North Atlantic.

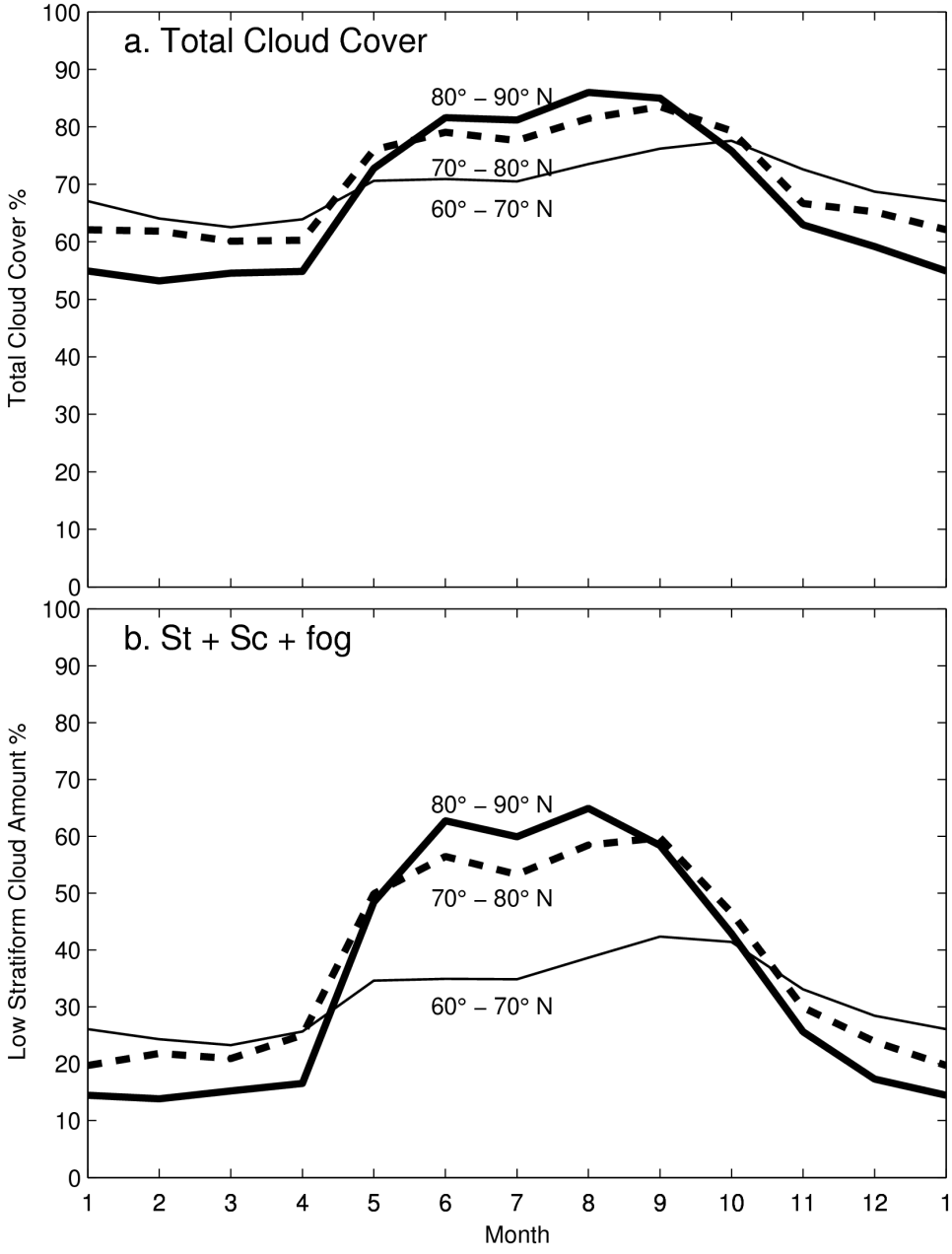

Figure 3, Annual Cycles of Cloud Cover by Latitude Band. a) The annual cycles of total cloud cover within 10˚ latitude bands in the Arctic. b) Annual cycles of stratiform cloud cover within the same latitude bands.

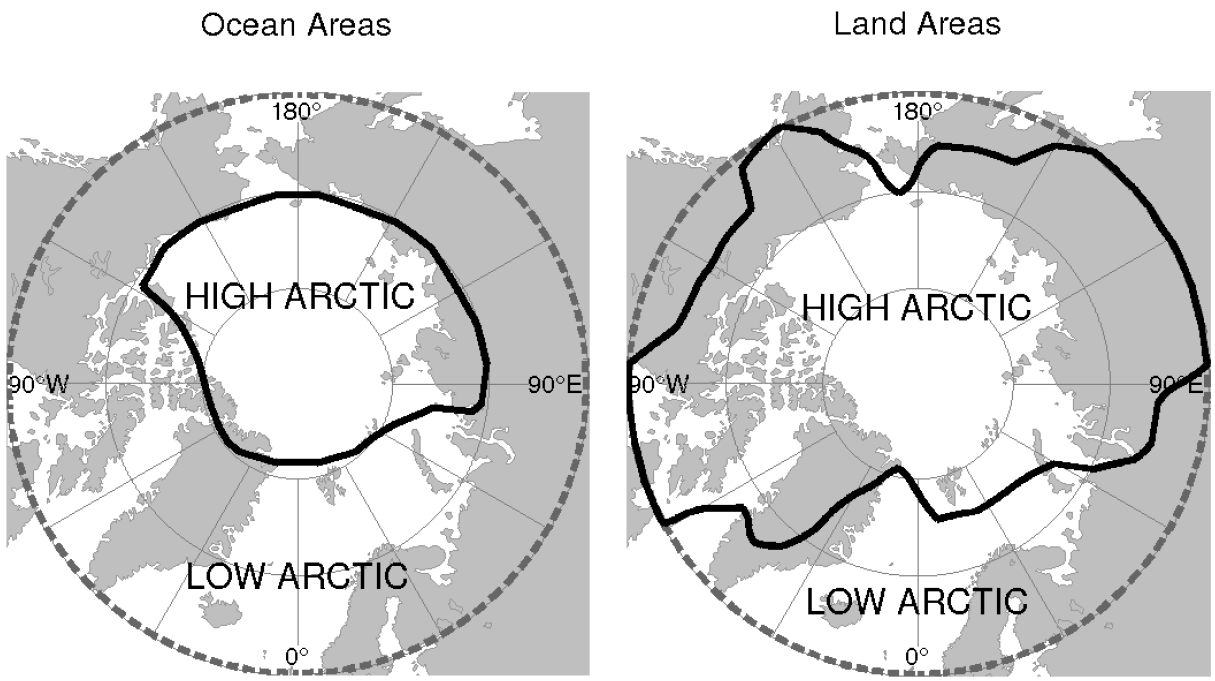

Figure 4, High and Low Arctic Boundary. Geographic boundary between the "Low Arctic" and "High Arctic" over land and ocean.

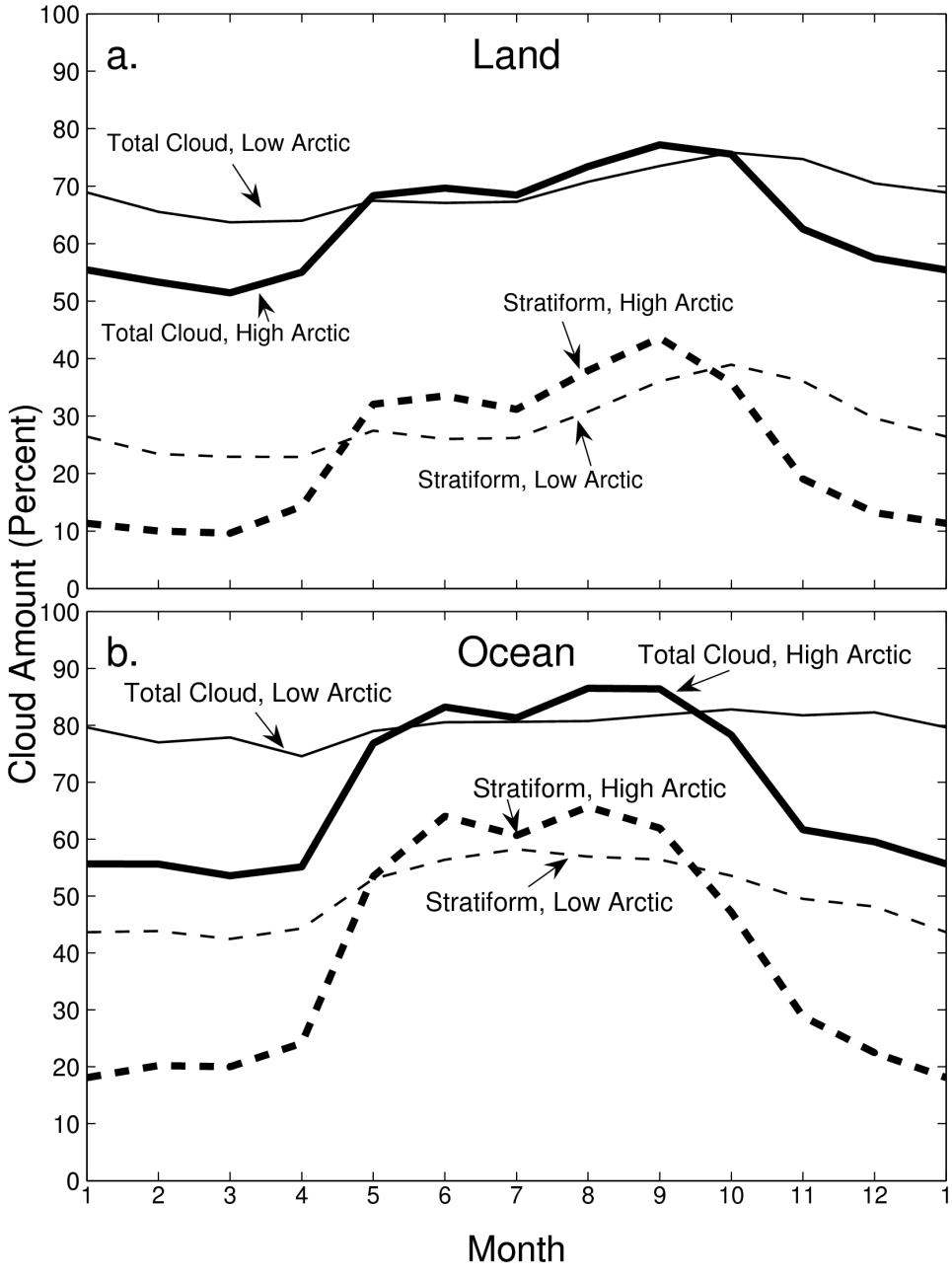

Figure 5, High and Low Arctic Seasonal Cycles of Total Cloud Cover and Stratiform Cloud Cover. The seasonal cycles of a) total cloud cover and b) stratiform cloud cover in the high and low Arctic over land and ocean.

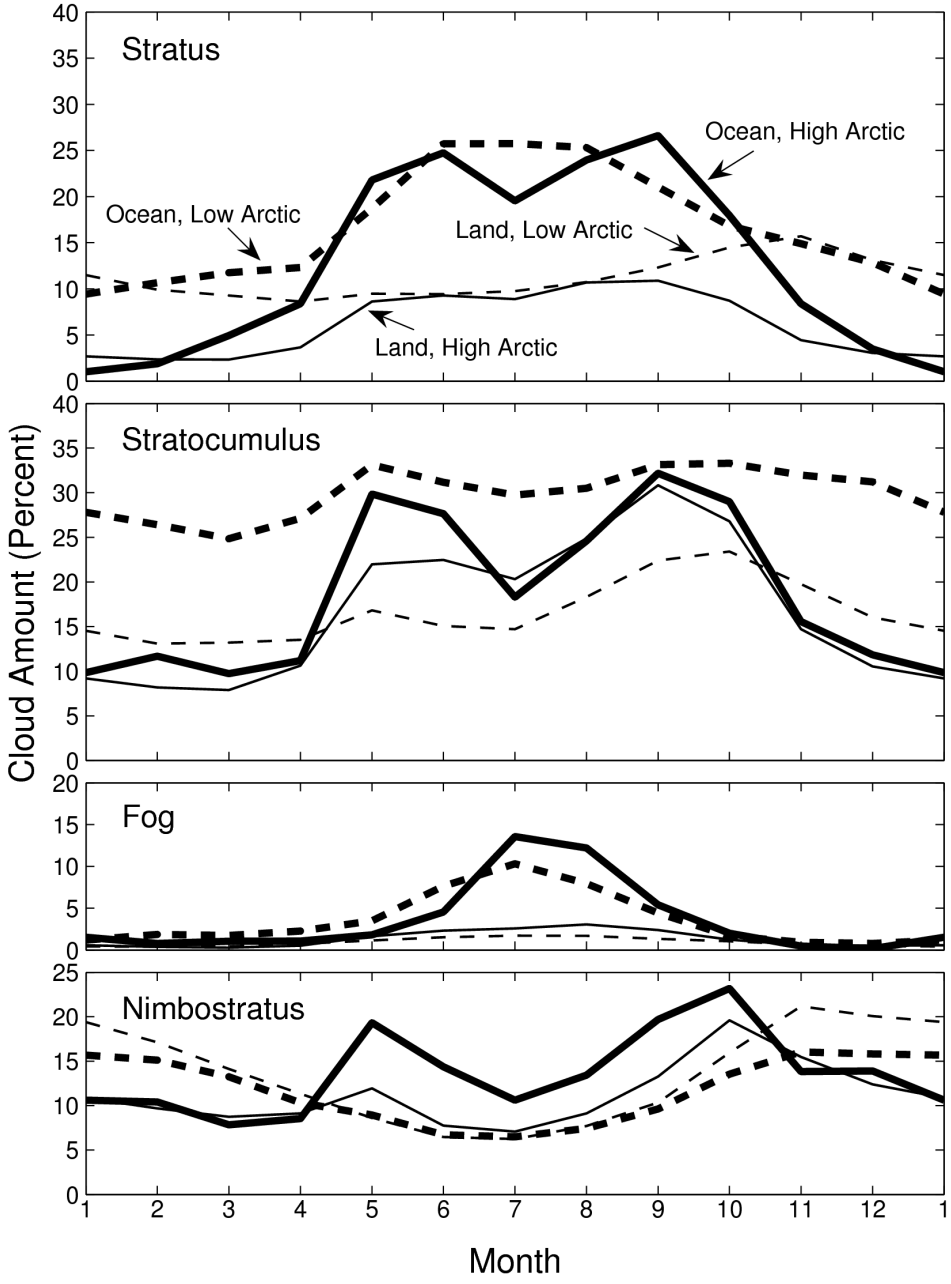

Figure 6, Seasonal Cycles of Low Stratiform Clouds. The seasonal cycles of low stratiform cloud types over land and ocean in the high and low Arctic.

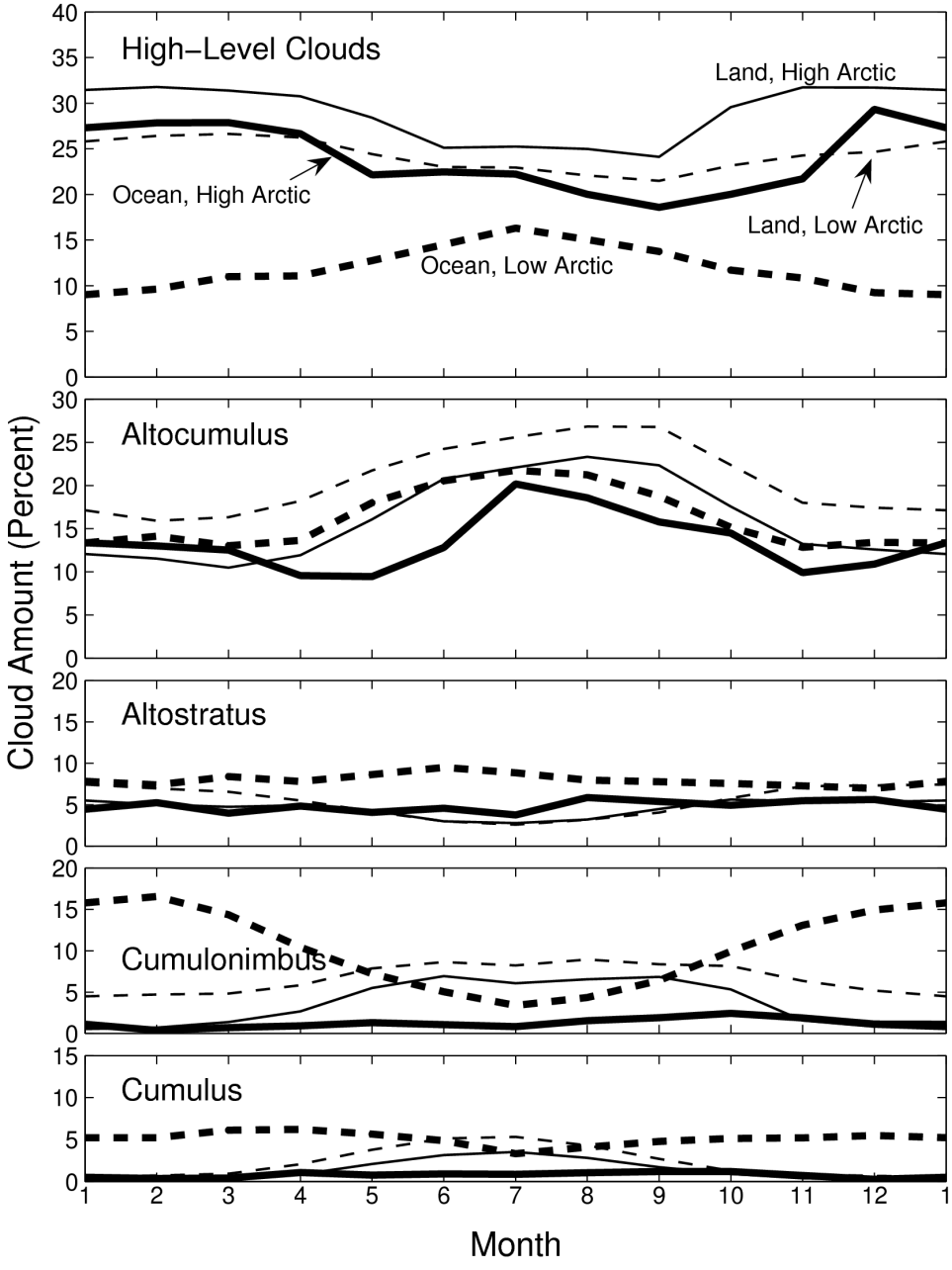

Figure 7, Seasonal Cycles of High, Middle, and Convective Clouds. The seasonal cycles of high, middle (As, Ac), and convective (Cu, Cb) clouds over land and ocean in the high and low Arctic.

Table 1, Arctic Cloud Amounts. Amounts (sky cover) of each cloud type, averaged over the region 60˚-90˚ N, weighted by grid box area and relative ocean and land area.

	Average Amount (%)									
	Land					Ocean				
Cloud type	DJF	MAM	JJA	SON	Annual	DJF	MAM	JJA	SON	Annual
Fog	0	1	2	1	1	1	2	9	2	4
Stratus (St)	6	7	10	10	8	9	13	25	18	17
Stratocumulus (Sc)	11	14	20	23	17	18	21	27	29	24
Cumulus (Cu)	0	2	4	1	2	3	3	3	3	3
Cumulonimbus (Cb)	2	4	7	6	5	8	5	3	6	5
Nimbostratus (Ns)	14	10	8	16	12	13	11	10	16	12
Altostratus (As)	6	5	3	5	5	6	6	7	6	6
Altocumulus (Ac)	14	15	23	20	18	12	12	19	15	15
High (cirriform)	29	28	24	26	27	16	17	18	16	18
Total Cloud Cover	60	61	70	73	66	66	70	82	79	75
Clear Sky (frequency)	22	18	7	10	14	12	11	3	5	8

4. TRENDS

Trend analysis is done for individual stations and grid boxes during all seasons across the Arctic in a way similar to that described in Warren et al. (2007). To reduce the effects of outliers on trends, the median of pairwise slopes method (Lanzante, 1996) is used to compute trends, but very similar results are obtained using the conventional least-squares method. A minimum of 50 observations per land station or ocean grid box per season per year is required for a seasonal cloud amount to be included in trend analysis. Over land, there must be a span of at least 20 years present, and within that span there must be a minimum of 15 individual years of data. Over the ocean, since the period of record is longer, a minimum span of 30 years is required with at least 25 individual years of data in each box. In order for a trend at an individual land station or ocean grid box to be considered significant the magnitude of the trend must exceed the standard deviation, or the standard deviation must be <2% per decade. Only trends considered significant by this criterion are plotted.

Figure 8 illustrates some geographic patterns of cloud trends over the Arctic. Trends displayed in both frames, in units of 0.1% per decade, represent combined land and ocean data spanning from 1971 to 2007. The trends are not uniform over the entire Arctic, but do appear to aggregate into large regions of

similar sign. These trends generally show little relationship with the boundaries of the high and low Arctic. For St in summer, figure 8a shows a large increase over the central Arctic and a weak decrease at lower latitudes. Figure 8b shows a different pattern in the geographic distribution of annual average trends of precipitating clouds. Positive trends are found over central Siberia and over the Canadian Arctic. A negative trend is apparent over much of northern Europe and coastal Asia as well as over Alaska and the entire Arctic Ocean. This negative trend of precipitating cloud (which is mostly Ns) is consistent with the negative trend of snow accumulation found by Warren et al. (1999). The Arctic mean trend shown at the base of the frames is the area-weighted mean of individual anomaly time series over the arctic land and ocean regions, which may differ from the mean of all numbers on the map. These two maps are just a sample. The complete set of maps for 12 types and 4 seasons, for land, ocean, and total area (144 maps total) will be available at our website: www.atmos.washington.edu/CloudMap.

Table 2 shows the average trend values for Arctic land, ocean, and combined land and ocean. These area-averaged trends are not particularly large, with magnitudes rarely exceeding 1% per decade. The trends are shown for total cloud cover, for 7 individual types, and for the combined types middle (As, Ac, Ns), low (St, Sc, fog, Cu, Cb), precipitating (Cb, Ns), and non-precipitating middle (As + Ac). As and Ac are combined here because their

individual trends are often opposing, which could be the result of a subtle change in observing procedure over time in how middle clouds are distinguished. The Arctic land trends (Table 2a) show an increase in overall cloud cover, but numerous trade-offs in types. Stratocumulus clouds tend to be increasing, but the other low stratiform clouds (St and fog), are decreasing. The precipitating type Ns is decreasing, but this decrease is being countered by a strong increase in Cb. These tradeoffs both indicate an increase of convective activity. The two precipitating types combine to make an overall positive trend over land. Mid-level clouds as a whole are increasing, driven by an increase in non-precipitating middle cloud cover.

Table 2b shows trends over the ocean for the 55-year period 1954 - 2008. The trends in total cloud cover are very weak and not significant in any season, but individual types do show interesting results. Oceanic low stratiform cloud cover tends to behave in the opposite manner to that over land. Stratus and fog are increasing while Sc is decreasing. Cumulonimbus is also behaving differently over the ocean, with significant decreases shown for all seasons. Nimbostratus is trending negatively during spring and summer, and only increasing during the winter. The combination of both precipitating cloud types produces a decreasing trend. Middle clouds are decreasing, once again in opposition to trends on land. For comparison, ocean trends have also been computed for the same time span as those over land, with little difference

between the longer and shorter spans. Over the shorter span, summer and autumn total cloud cover do show significant increases, and the decrease in Sc and increase in fog are less significant, but otherwise little change is seen in types when comparing trends for the different time periods.

In Table 2c, the trends in cloud cover over the entire Arctic are shown. These are computed by area-weighting the land and ocean anomalies to form an average anomaly, and fitting a trend line to the time series of average anomalies. The overall trends show a slight but significant positive trend in total cloud cover in all seasons. This trend is strongest during spring and autumn. The increase appears primarily driven by increasing low cloud cover, and is partially countered by a decrease in precipitating cloud amount. These changes are likely a complex feedback associated with the large-scale changes observed in Arctic climate. The impact of these cloud changes is likely to increase downward longwave CRE, leading to a net warming in winter, spring and autumn. The observed decrease in precipitating cloud cover, and the likely accompanying decrease in snowfall, may be acting to enhance ice melt in summer by decreasing the surface albedo.

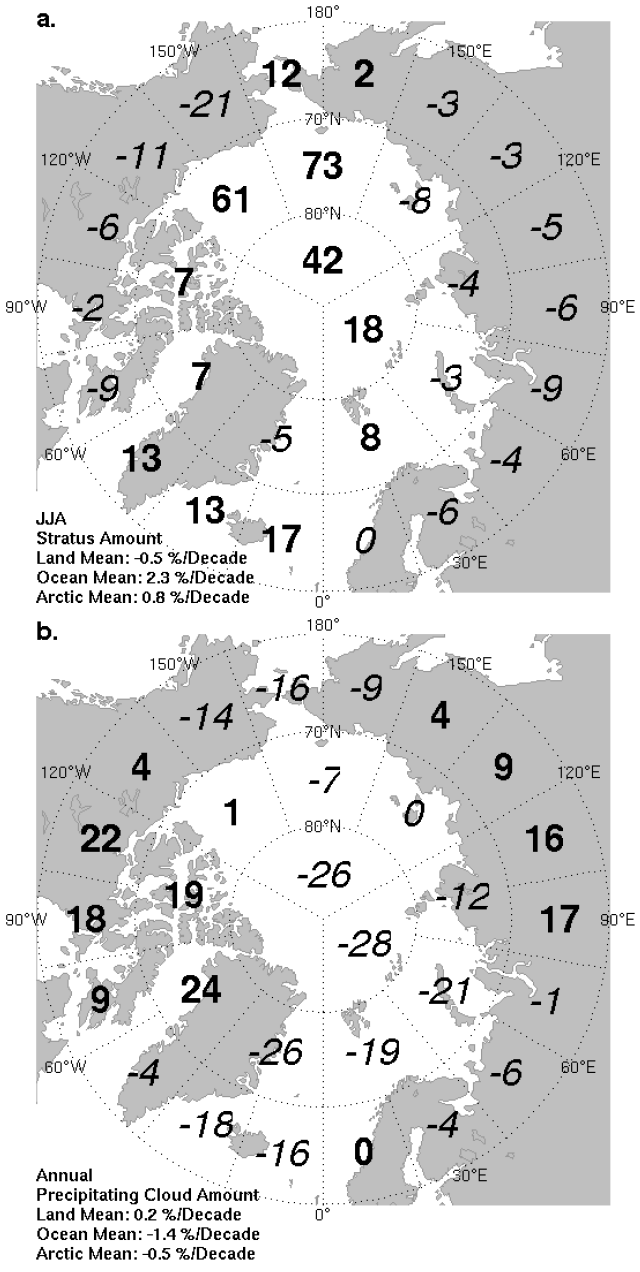

Figure 8, Geographic Distribution of Trends. Trends (0.1% / Decade) of a) summertime stratus cloud amount and b) annual mean precipitating (Ns + Cb) cloud amount in grid boxes representing land and ocean areas.

Table 2, Trends of Cloud Amounts. Trends in Arctic cloud amounts (percent per decade), from linear fits to seasonal averages.

a) Arctic Land Trends (1971 -2007)

	Total	St	Sc	Fog	Cu	Cb	Ns	As + Ac	High	Middle	Low	Precipitating
DJF	**0.5**	**-0.5**	**1.3**	**-0.1**	0.1	**0.3**	0.0	**0.3**	0.0	**0.2**	**1.2**	**0.2**
MAM	**0.6**	**-0.5**	**1.1**	**-0.1**	0.0	**0.5**	**-0.3**	**0.7**	**-0.2**	**0.5**	**1.1**	**0.3**
JJA	**0.3**	**-0.5**	**0.4**	**-0.2**	**-0.1**	**0.6**	**-0.4**	**0.6**	**0.3**	**0.2**	0.2	**0.2**
SON	**0.4**	**-0.8**	**0.9**	**-0.1**	0.1	**0.7**	**-0.4**	**0.9**	**-0.2**	**0.5**	**1.0**	**0.3**

b) Arctic Oceanic Trends (1954-2008)

	Total	St	Sc	Fog	Cu	Cb	Ns	As + Ac	High	Middle	Low	Precipitating
DJF	0.1	**1.5**	**-0.7**	**0.1**	**0.2**	**-1.1**	**0.4**	**-1.0**	0.0	**-0.5**	0.2	**-0.7**
MAM	**-0.3**	**1.1**	**-0.4**	**0.3**	**0.6**	**-1.1**	**-0.4**	**-0.7**	**-0.4**	**-1.1**	**0.3**	**-1.6**
JJA	-0.1	**1.3**	**-0.7**	**0.2**	**0.4**	**-0.3**	**-0.5**	-0.2	**0.3**	**-0.4**	**0.9**	**-0.8**
SON	0.0	**1.2**	-0.2	0.0	**0.5**	**-0.6**	-0.1	-0.2	0.0	**-0.8**	**0.9**	**-0.7**

c) Arctic Trends (1971 -2007)

	Total	St	Sc	Fog	Cu	Cb	Ns	As + Ac	High	Middle	Low	Precipitating
DJF	**0.3**	0.2	**0.8**	0.0	**0.1**	**-0.5**	0.2	**-0.6**	0.2	0.0	**0.8**	**-0.4**
MAM	0.2	**0.5**	**0.3**	0.0	**0.2**	**-0.4**	**-0.4**	0.0	**-0.5**	**-0.4**	**0.7**	**-0.9**
JJA	**0.2**	**0.8**	**-0.3**	0.0	**0.1**	0.0	**-0.4**	**0.3**	**0.2**	0.0	**0.7**	**-0.4**
SON	**0.5**	**0.8**	**0.5**	**-0.1**	**0.3**	**-0.2**	**-0.2**	**0.6**	-0.2	0.0	**1.4**	**-0.5**

5. CLOUDS AND ARCTIC SEA ICE

To specifically study the relationships between cloud cover and sea ice, composite time series have been analyzed using a variety of methods for two regions, (a) the Arctic Ocean as a whole and (b) the region of large recent sea ice anomalies, extending from the Laptev Sea, through the East Siberian and Chukchi Seas, to the Beaufort Sea. This latter region we call "Beaufort-Laptev" (B-L) for short. These regions are shown on the map in Figure 9. The Arctic Ocean region contains all ocean area north of 80° N between 120° W and 80° E and all ocean north of 70° N from 80° E to 120° W. The Arctic Ocean region also includes all land-based synoptic stations bordering the Arctic Ocean between 80° E and 120° W, but excluding stations along the Chukchi Sea south of 70° N. The B-L region is similar to the region studied by Schweiger et al. (2008); it represents the region where the sea-ice margin shows the most variability, which should ideally show a strong cloud precursor or response associated with changes in ice extent. This region has the same coastal border as the Arctic Ocean, but is bordered on its west by 120° E, on its east by 120 ° W, and to the north by 80° N.

A trend analysis of all cloud types has been done for these regions. We will show figures for only the most significant results. We correlate the interannual variations of cloud types with surface and upper air temperatures,

total sea ice extent, and the Arctic Oscillation index (Thompson & Wallace, 1998). A superposed epoch study is also done using the difference between cloud amounts for each type during the five years with the least and the five years with greatest sea ice extent. Results from the correlation analyses and superposed epoch study are shown in tables.

a. Trends

Selected time series of cloud cover anomalies are shown in Figure 10 for the Arctic Ocean and in Figure 11 for the B-L region. Trend lines are computed; a trend is considered significant if its magnitude exceeds its standard deviation.

Significant positive trends of total cloud cover are found in three of the four seasons over the B-L, and two of four over the Arctic Ocean (Figures 10a, 11a). Only wintertime lacks a significant trend in either region, though both regions do exhibit a slight increase. In springtime (MAM), the largest trend in total cloud cover is observed over the B-L, while in autumn (SON) the trend is greatest over the entire Arctic Ocean. Spring and autumn display the largest increase in both regions with more modest increases during summer and winter.

Trends in individual cloud types tend to keep their sign throughout the year rather than show different tendencies between seasons. Figures 10b and 11b show low clouds increasing year round, and this increase is being countered by a consistent, strong decrease in precipitating clouds (mostly Ns,

but also Cb, Figures 10c and 11c) and fog. The positive trend of low cloud amount, which appears to be the primary driver for the total cloud cover trend, is mainly the result of increases in low stratiform cloud cover. The type of low stratiform cloud cover that is changing differs between regions with mainly stratus increasing over the Arctic Ocean (Figure 10d), but stratocumulus increasing over the B-L (Figure 11d).

Overall, trends in cloud cover show increasing cloud cover over the Arctic Ocean as a whole and over the B-L region. The increasing trend is most substantial during spring and autumn. This result is consistent with observed trends in sea ice if the climate models are correct in predicting that increasing clouds during SON, DJF, and MAM will decrease ice thickness. Looking further at types shows a decrease in precipitating clouds and corresponding increase in non-precipitating, low stratiform clouds. One possible explanation for this change from precipitating to non precipitating cloud might be greater aerosol loading creating smaller cloud droplets resulting in longer-lived clouds that fail to precipitate. This is unlikely, however, since Quinn et al. (2007) have shown a decreasing trend in Arctic sulfate aerosols. A different cloud type is responsible for the increase in low stratiform cloud cover when comparing the entire Arctic Ocean and the B-L. The increase in Sc instead of St in the B-L may be the result of changing boundary-layer characteristics associated with decreasing ice cover, which has been attributed to decreasing static stability as discussed by

Schweiger et al. (2008). Observed decreases in fog further substantiate the idea of decreasing stability. The decrease in precipitating clouds, and therefore a likely decrease in snowfall, may also play a role in the observed decrease in September ice extent and thickness by reducing the albedo of the sea ice surface in summer and causing more rapid melt.

b. Correlations

Cloud cover anomalies are correlated with September sea ice extent anomalies, seasonal temperature anomalies over the Arctic Ocean and B-L region, and the Arctic Oscillation index. The correlations are done with both detrended and unaltered time series in order to assess the reliability of our results. Tables are shown only for the unaltered time series since most relationships remained intact regardless of detrending. Some correlation coefficients (r-values) do change sign when detrended data are correlated, though never from a significant positive to significant negative or vice-versa. Correlations are considered significant at a 95% level; significant correlations are shown in bold print on the accompanying tables.

Correlation coefficients between September sea ice extent and total cloud cover during all seasons of the same year are displayed in the leftmost column of Table 3. A significant negative correlation between cloud cover and ice extent is present during spring and autumn, indicating that lower than average

autumn ice extent is associated with increased cloudiness over the ice. In both winter and summer there are weaker, but still negative, correlations. During summer, we expected the sign of the correlation to change to positive due to the dominance of shortwave CRE, and these values alone change sign when the time series are detrended. We have to conclude that summertime cloud cover is uncorrelated with September sea ice extent, but there may be significant correlation with individual cloud types.

Low clouds appear to be the major contributor to the pattern of correlations shown for total cloud cover, specifically low types St and Cb, which correlate negatively throughout the year with September ice extent. September sea ice extent correlates positively with summertime Sc and precipitating clouds, especially Ns. The relationship between precipitation and ice extent is strongest during summer, though over the B-L it is present from winter through summer.

Table 4 shows correlations of cloud amounts with seasonal surface air temperature (SAT) anomalies as determined by the NCEP/NCAR reanalysis (Kalnay et al., 1996). Positive correlations are found in winter, spring, and autumn. In summer the correlation is negative but insignificant. A likely reason for the weak correlation during summer is the lack of variability in summertime SAT over melting ice. When correlations are made using reanalysis temperatures at 850 and 500mb, the summertime negative correlation with air

temperature becomes significant.

Low clouds, specifically stratus, drive the positive correlation during autumn, but in winter and spring the non-precipitating middle clouds also contribute. SAT correlates well with the non-precipitating middle clouds, but at higher levels this relationship weakens, though does not change sign. This is not true for low clouds, which correlate just as well with temperatures at 850 and 500 mb. Stratocumulus and precipitating clouds are associated with cooler temperatures at all levels during summer, but for the remainder of the year precipitation shows little relationship with temperature.

Total cloud cover is also correlated with the seasonal Arctic Oscillation (Table 5). A positive AO is associated with lower pressure over the Arctic, a strong jet stream shifted slightly northward, and a colder stratosphere. In spring and summer, the AO and total cloud cover correlate positively, and the correlations are significant for the time series over the entire Arctic Ocean. In autumn, the correlation is negative and significant over the B-L, but not over the Arctic Ocean as a whole. The wintertime correlation is not substantial for either region. Interestingly, trends in the arctic oscillation are positive in all seasons except autumn, and though these trends are very small, they suggest that changes in circulation due to the AO could be acting to increase cloud cover throughout much of the year. Variations in cloud types do not correlate as strongly with the AO as with other variables. The AO appears to have a

stronger relationship with middle and high clouds overall, with positive correlation during spring and summer, and with precipitating clouds, which correlate positively only during summer.

Also of interest in this study are correlations among the three variables whose correlations with clouds we have examined: Ice extent, SAT anomalies, and the Arctic Oscillation. A consistent negative correlation is present between surface air temperature anomalies and September ice extent during spring, summer and autumn, indicating that a warming surface does lead to thinning ice. The AO index and September sea ice extent show no significant correlation, though the largest values were negative during winter and spring. These negative correlations suggest that a positive Arctic Oscillation during winter and spring can be associated with a reduction in sea ice extent in the following September. The Arctic Oscillation and Arctic Ocean SAT show little to no relationship in winter and summer, but a positive correlation in spring, and a significant negative relationship in autumn, suggesting that a positive AO in the springtime is associated with warmer temperatures, while a positive AO during autumn is associated with cooling.

c. Superposed Epochs

Two subsets of cloud anomaly data are chosen based on September sea ice extent between 1979 and 2007 (consistent data on sea-ice extent are

available beginning in 1979). In this case, cloud cover anomalies during the five years with the most September sea ice and the five years with the least are compared. Anomalies are averaged for each of the five-year subsets, and the mean cloud anomaly for the high-ice years is subtracted from the mean anomaly for the low-ice years to produce a difference of mean cloud cover (DMCC). A student's t-test is done to determine whether the DMCC is significant. Due to the limited number of data points available, a significance level of 90% has been chosen. A positive DMCC indicates that cloud cover of that specific type is higher during years with less September sea ice, and a negative DMCC means the opposite. Because of the declining trend of Arctic Sea Ice, the low-ice years are all post-2000 and the high-ice years are all pre-2000 (Figure 12).

This analysis has been done over the B-L as well as entire Arctic Ocean region for all cloud types during all seasons in the year of the ice extent anomaly, plus the preceding winter (Table 6). All DMCC values for total cloud cover during all seasons analyzed are positive, with statistically significant values during autumn for both regions. Analyzing cloud types shows that low clouds, particularly stratus clouds, are the cause of the greater autumn cloud cover during a low-ice year, with low-cloud amounts greater by more than 10%. Figure 12b shows the autumn time series over the B-L of low cloud cover with high and low ice years indicated. Precipitating clouds showed a less substantial

relationship than in the analyses of the previous section, but the overall pattern of more summer precipitating clouds during high-ice years has stayed intact.

This analysis shows that the total cloudiness during autumn of a low-ice year is significantly greater than that of a high-ice year. All five of the low-ice years had greater SON cloud cover than any of the high-ice years. This implies a response of increased cloud cover to increased areal coverage of open water over the Arctic. Summer precipitation also appears to produce a slight positive response in September sea ice extent. As a whole, years with less ice extent generally have more cloud cover, especially in non-summer seasons, though most of the differences were not large enough to be considered statistically significant with this limited range of data.

d. Discussion

This study of Arctic Ocean cloud cover indicates that increases in Arctic cloud cover are generally associated with decreased sea ice and warmer temperatures. These relationships are true over the B-L region where maximum variability in ice exists and remain significant over the entire Arctic. Correlations with temperature and sea ice extent are strongest during spring and autumn when longwave dominates. It is shown that low clouds have a strong positive relationship with temperature during these seasons. Precipitating clouds appear to be associated with cooling during summer and

subsequently with increased September sea ice extent. A clear cloud response to changing sea ice is observed as low cloudiness tends to increase substantially during autumn following a particularly low September ice extent.

Observed trends in cloud cover appear to act to enhance the effects of Arctic warming in both regions studied. Increasing low stratiform cloud cover during spring and autumn should increase the warmth associated with those cloud types during those seasons. The substantial decrease observed in precipitating clouds should reduce snow cover, causing reduced surface albedo throughout the summer. Increasing stratiform cloud cover, and the accompanying decrease in precipitating clouds, suggests a possible link with aerosols. This aerosol effect would decrease cloud droplet size and increase number densities as aerosols increase, as was observed by Garrett and Zhao (2006). This would act to prolong the life of a cloud and reduce precipitation, as well as increase the emissivity of the cloud. However, the trend of Arctic aerosols has gone in the opposite direction, as Quinn et al. (2007) have observed decreasing sulfate aerosols since the mid 1990's at surface stations in the Arctic. Finally, relationships between circulation changes associated with the Arctic Oscillation and cloud cover appear somewhat weak on this large scale, however trends found in the Arctic Oscillation index may have a slight effect, increasing cloud cover throughout the year.

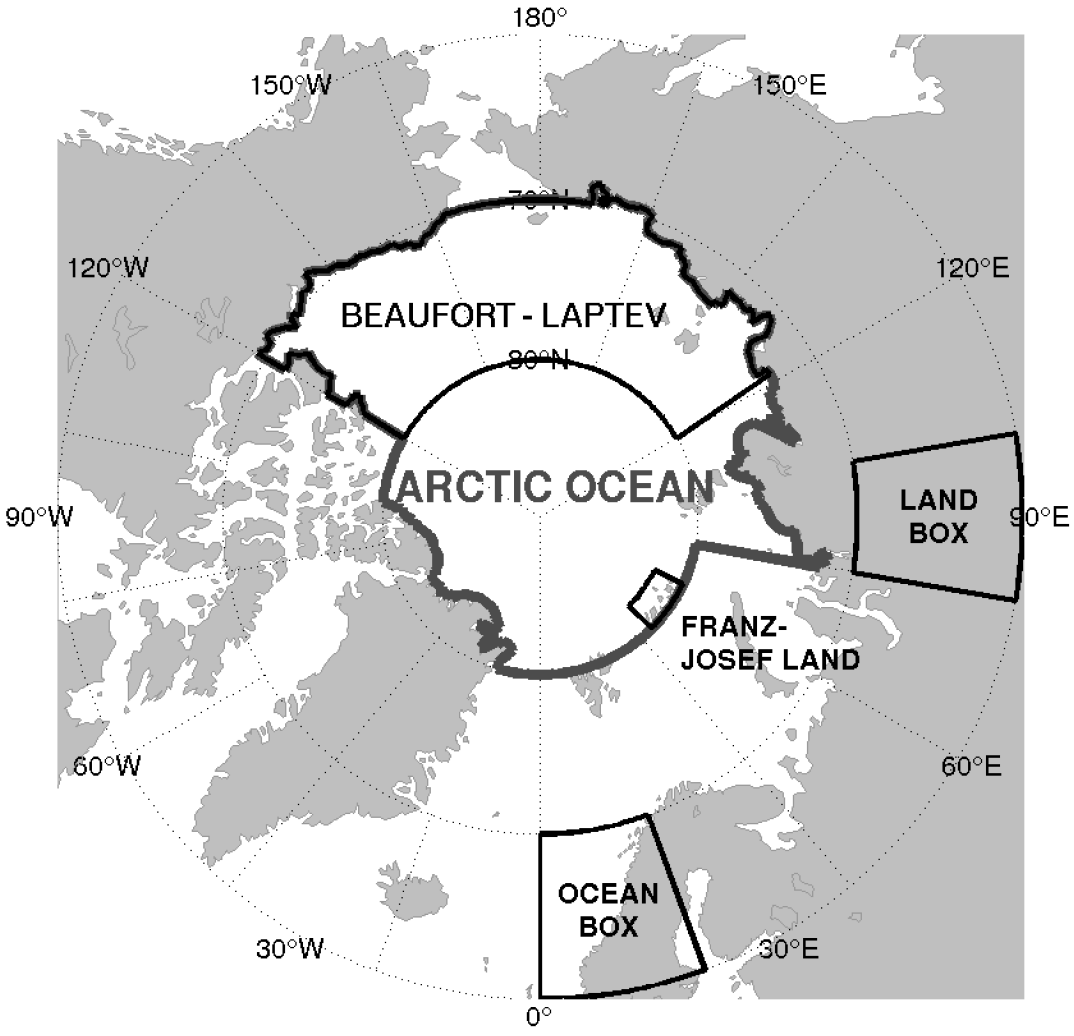

Figure 9, Sub-Regions Within the Arctic. Sub-regions within the Arctic defined for comparisons of clouds with other variables. Also shown are three boxes used for a comparison with satellite data in Chapter 6.

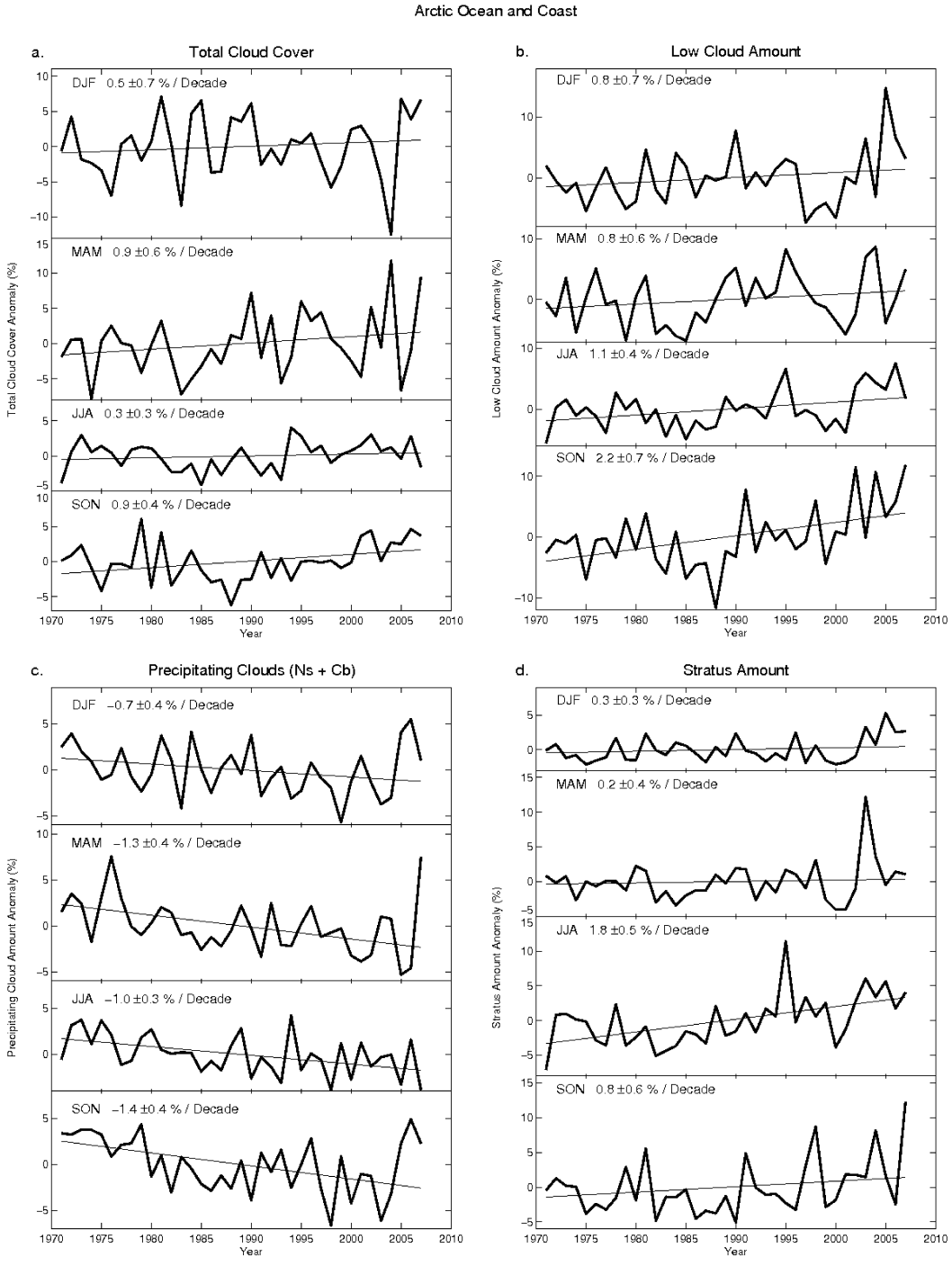

Figure 10, Seasonal Anomaly Time Series over the Arctic Ocean and Coast. Time series of seasonal anomalies of a) total cloud cover, b) low cloud amount, c) precipitating cloud amount and d) St cloud amount over the Arctic Ocean and coast.

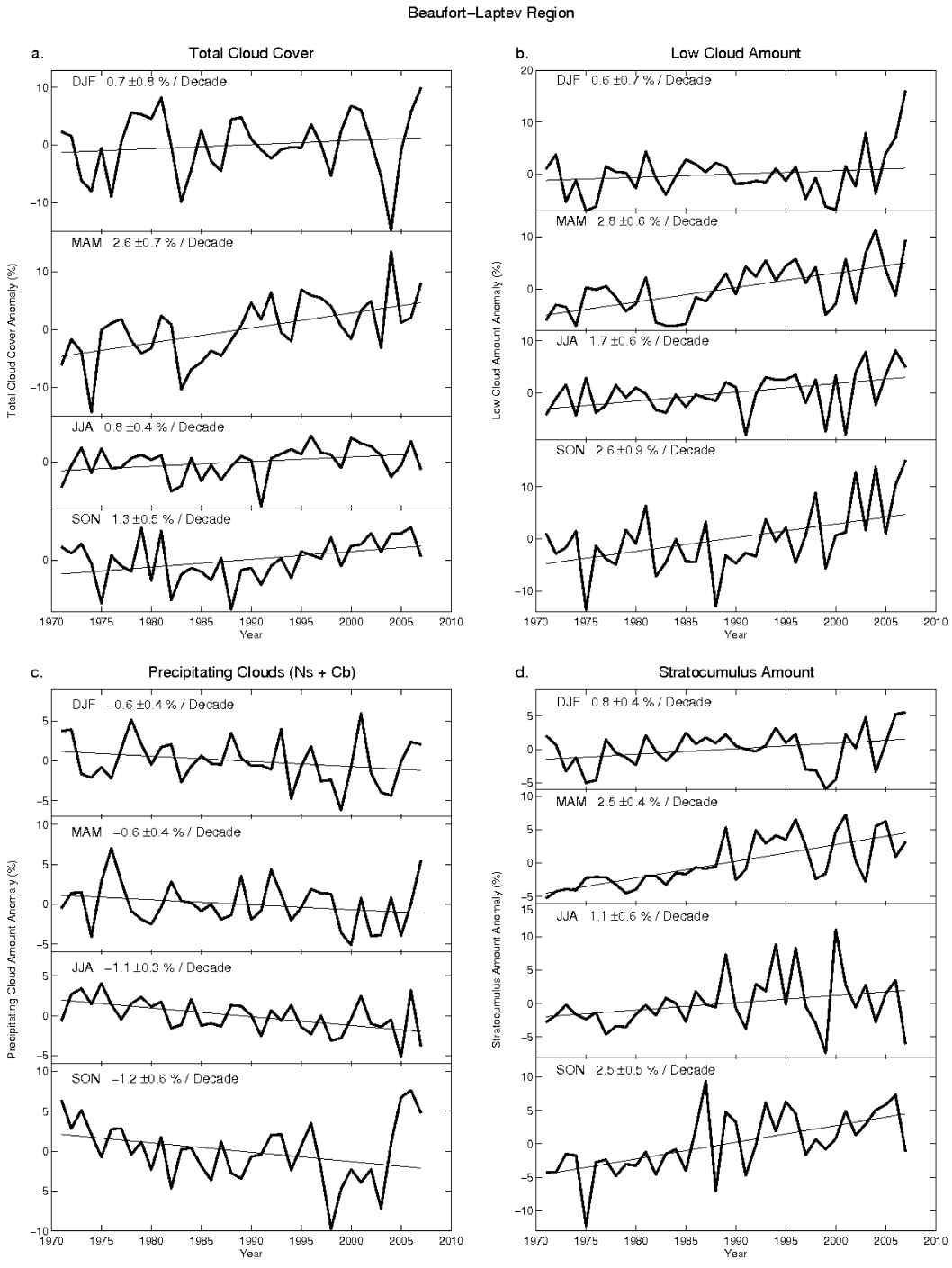

Figure 11, Seasonal Anomaly Time Series over the Beaufort-Laptev. Time series of seasonal anomalies of a) total cloud cover, b) low cloud amount, c) precipitating cloud amount and d) Sc cloud amount over the Beaufort-Laptev.

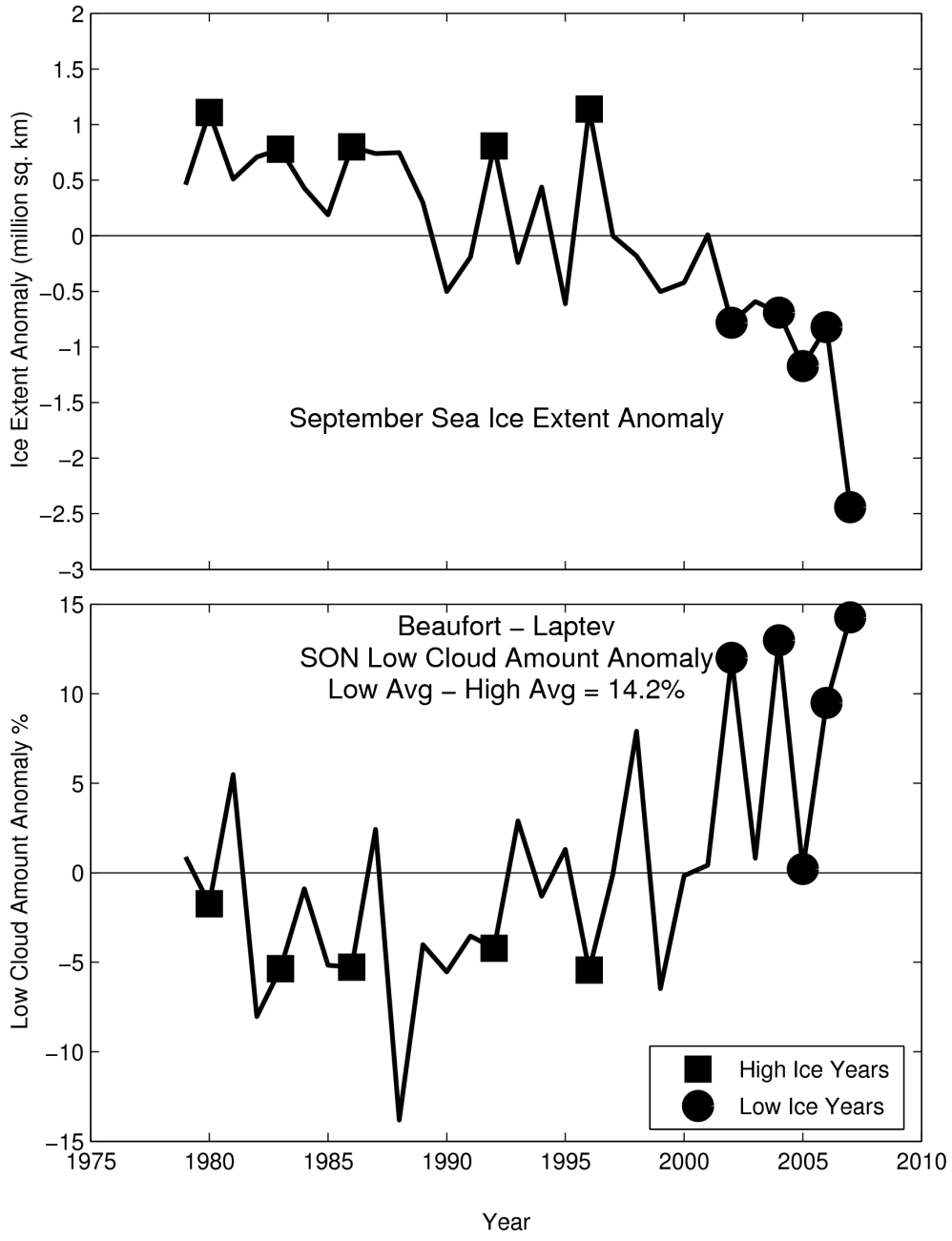

Figure 12, Time Series of Sea Ice Extent and Autumn Low Cloud Cover. Time series of September Arctic sea ice extent anomaly (top) with high and low ice years shown and (bottom) the accompanying time series of autumn low cloud cover anomaly showing cloud amounts during high and low ice years.

Table 3, Correlation Analysis Results: Sea Ice Extent. Correlation coefficient of seasonal average cloud amount with September Arctic sea-ice extent in the same year.

a) **Arctic Ocean Region**

	Total	St	Sc	Fog	Cu	Cb	Ns	As + Ac	High	Middle	Low	Precipitating
DJF	-0.2	**-0.4**	-0.2	0.3	0.1	**-0.5**	0.0	0.1	0.1	0.1	-0.3	-0.1
MAM	-0.4	-0.3	-0.1	0.0	0.1	-0.3	0.1	-0.1	-0.2	0.0	-0.3	-0.1
JJA	-0.1	**-0.6**	**0.5**	-0.2	-0.1	-0.1	**0.5**	0.2	0.0	**0.5**	**-0.5**	**0.5**
SON	**-0.5**	**-0.5**	-0.2	-0.3	-0.3	-0.3	0.1	-0.3	0.2	0.0	**-0.7**	-0.1

b) **Beaufort - Laptev Region**

	Total	St	Sc	Fog	Cu	Cb	Ns	As + Ac	High	Middle	Low	Precipitating
DJF	-0.1	**-0.5**	-0.2	0.3	0.0	**-0.6**	0.3	0.0	-0.2	0.2	**-0.4**	0.1
MAM	**-0.5**	-0.2	-0.3	0.0	-0.1	**-0.5**	0.4	0.0	-0.3	0.2	**-0.4**	0.1
JJA	-0.1	**-0.5**	0.3	0.0	**-0.4**	-0.2	**0.6**	0.2	-0.1	**0.4**	-0.3	**0.4**
SON	**-0.5**	**-0.4**	-0.3	-0.1	**-0.5**	**-0.5**	0.0	-0.2	0.2	0.1	**-0.6**	-0.3

Table 4, Correlation Analysis Results: Temperature. Correlation coefficient of seasonal average cloud amount with seasonal average surface air temperature.

a) Arctic Ocean Region

	Total	St	Sc	Fog	Cu	Cb	Ns	As + Ac	High	Middle	Low	Precipitating
DJF	**0.5**	**0.5**	**0.5**	0	0	0.1	0.3	0.3	-0.2	**0.4**	**0.6**	0.3
MAM	**0.5**	**0.5**	**0.4**	-0.2	0	-0.1	0	**0.4**	0	0.3	**0.6**	0
JJA	-0.1	**0.4**	**-0.4**	0.3	0.1	-0.1	**-0.5**	-0.3	0	**-0.5**	**0.3**	**-0.5**
SON	**0.6**	**0.6**	0.3	0.1	0.2	0.1	-0.2	**0.5**	**-0.4**	0.1	**0.7**	-0.1

b) Beaufort - Laptev Region

	Total	St	Sc	Fog	Cu	Cb	Ns	As + Ac	High	Middle	Low	Precipitating
DJF	**0.4**	**0.3**	**0.3**	0.2	0	0.1	0.1	**0.4**	0.1	0.3	**0.4**	0.1
MAM	**0.5**	**0.4**	**0.3**	-0.1	0.2	0.2	-0.3	**0.4**	0.2	0.1	**0.6**	-0.2
JJA	-0.2	0.3	-0.3	0.1	0.3	-0.1	**-0.5**	-0.2	0.1	**-0.4**	0.1	**-0.5**
SON	**0.6**	**0.4**	**0.3**	0.1	**0.4**	0.3	-0.1	0.3	-0.2	-0.1	**0.7**	0.1

Table 5, Correlation Analysis Results: Arctic Oscillation. Correlation coefficient of seasonal average cloud amount with seasonal average Arctic Oscillation index.

a) Arctic Ocean Region

	Total	St	Sc	Fog	Cu	Cb	Ns	As + Ac	High	Middle	Low	Precipitating
DJF	0.1	-0.1	0.1	**-0.3**	0.2	0.2	0.0	-0.1	**0.3**	0.0	0.0	0.0
MAM	**0.4**	0.1	0.2	0.1	0.0	0.2	0.2	0.3	**0.6**	**0.4**	0.2	0.3
JJA	**0.5**	0.0	**0.3**	-0.2	0.1	0.2	**0.5**	0.2	0.2	0.3	0.2	**0.5**
SON	**-0.4**	-0.3	-0.1	**-0.3**	-0.3	-0.1	0.1	**-0.4**	0.2	-0.2	**-0.4**	0.1

b) Beaufort - Laptev Region

	Total	St	Sc	Fog	Cu	Cb	Ns	As + Ac	High	Middle	Low	Precipitating
DJF	0.0	-0.2	-0.2	**-0.4**	0.1	0.2	-0.2	-0.1	**0.3**	-0.2	-0.2	-0.2
MAM	0.3	0.1	0.0	0.0	-0.1	0.2	0.1	0.2	**0.5**	0.2	0.1	0.2
JJA	**0.3**	-0.2	**0.5**	**-0.4**	0.0	0.1	0.3	0.2	**0.3**	0.3	0.1	0.3
SON	**-0.4**	**-0.4**	-0.1	**-0.4**	-0.3	-0.1	0.1	**-0.3**	0.1	-0.1	**-0.5**	0.0

Table 6, Superposed Epochs Results. Difference of mean seasonal cloud amount: Low-ice years minus high-ice years.

a) Arctic Ocean Region

	Total	St	Sc	Fog	Cu	Cb	Ns	As + Ac	High	Middle	Low	Precipitating
DJF (previous)	3.1	2.2	3.2	**-0.1**	-0.1	0.5	2.2	-0.9	-3.5	1.6	5.7	2.7
MAM	4.0	1.3	0.0	-0.3	-0.5	0.5	-2.0	-0.7	2.6	-2.8	1.1	-1.5
JJA	**1.5**	**5.7**	-3.2	2.1	0.4	0.5	-2.0	-4.5	2.3	**-6.8**	**5.3**	-1.6
SON	**5.6**	**6.5**	2.0	**0.8**	0.7	2.0	-0.7	2.1	-0.7	-1.6	**12.0**	1.3
DJF (following)	2.5	**3.8**	3.3	**-0.1**	0.0	0.6	-0.4	-1.7	-2.0	-1.5	**7.6**	0.2

b) Beaufort – Laptev Region

	Total	St	Sc	Fog	Cu	Cb	Ns	As + Ac	High	Middle	Low	Precipitating
DJF (previous)	1.5	2.5	2.0	-0.2	0.0	0.9	-0.7	0.3	-0.6	-0.4	5.1	0.2
MAM	6.9	1.0	2.5	-0.2	-0.1	1.5	**-2.7**	-0.7	4.0	-3.4	4.8	-1.1
JJA	0.2	4.1	-3.4	0.9	0.8	1.2	**-2.1**	-5.7	3.5	**-7.9**	3.6	-1.0
SON	**6.0**	5.7	**3.3**	0.6	1.2	**3.4**	0.3	0.6	0.6	-2.8	**14.2**	3.6
DJF (following)	2.5	**4.4**	**3.9**	-0.3	-0.1	1.2	-1.5	-1.7	1.5	-3.2	**9.1**	-0.3

6. COMPARISON WITH SATELLITE DATA

Recent publications (Schweiger 2004, Warren et al. 2007, and Wang and Key 2005) have shown conflict concerning trends in total cloud cover over the Arctic. In order to better understand the differences present between data sets, total cloud cover from the two satellite-derived data sets has been compared to surface observations over the Arctic. The AVHRR Polar Pathfinder extended (APP-x) data covers the entire Arctic on the 25 km EASE grid beginning in 1982, and are currently available through 2004. Data from the TIROS Operational Vertical Sounder (TOVS) are available on the 100 km EASE grid from 1980 through 2005. Because previous work with the TOVS data set has focused on clouds detected over ocean areas only, this study will also use only ocean area for the Arctic average time series of TOVS data. TOVS data over land are used later in this section.

We begin with a comparison of yearly total cloud cover anomalies over the entire Arctic. Yearly anomalies in APP-x data represent all area north of 60° N, while anomalies for the TOVS data are for ocean areas only. Figures 13 and 14 show these anomaly time series plotted along with anomalies of surface observed total cloud cover over the same regions. The slopes of trend lines (median of pairwise slopes) are given in the figures, fitted for the overlapping time period only. Linear correlation coefficients are shown for the detrended

time series as well as for the unaltered data in order to test for any bias associated with instrument-induced spurious trends.

In Figure 13, trends in APP-x data agree in sign and relative magnitude with surface observations only during summer and spring. During autumn and winter trends and trend magnitudes differ substantially. In both the autumn and winter cases there is a strong negative trend present in the APP-x time series, but a weak positive trend in surface observed clouds. The intarannual variations (IAVs) are also much larger in the APP-x data in autumn and winter. During spring and summer, APP-x trends show IAVs more similar to those of the surface observations. The r-value in summer is very weakly positive, and due to the influence of a few points near the beginning of the APP-x time series, the spring correlation coefficient is negative. However, when the spring time series are visually compared some agreement in variation is seen throughout much of the overlapping period. Correlation between surface observations and the APP-x data in winter and autumn is weakly negative.

In the APP-x dataset, the magnitude of IAVs is much larger in the dark seasons (autumn and winter) than in the sunlit seasons, but in the surface observations the IAVs for all seasons are similar (Figure 13). This suggests, but does not prove, that the discrepancy in dark-season trends is caused more by error in the APP-x than by error in the surface observations.

Total cloud cover trends over the ocean areas of the Arctic from TOVS

data (Figure 14) agree in sign with those derived from surface observations during spring and autumn. The springtime trend in the TOVS is an order of magnitude larger than the trend in surface-observed clouds and, as was the case in the APP-x data, the wintertime IAV is much greater for the TOVS. The summertime TOVS trend shows a larger uncertainty than that from APP-x or surface observations, mainly due to large negative anomalies in 1985 and 1997, which do not coincide with any strong downward spikes in APP-x data or the surface observations. During summer the correlations between TOVS data and surface observations are slightly positive. However, during spring, autumn and winter the correlations are essentially zero.

The differences in cloud variations among these data sets could result from insufficient numbers of surface observations, satellite-based detection errors associated with day versus night cloud detection, inversions of varying strength interfering with remote sensing of temperature profiles, or cloud detection over surfaces of different albedo. To investigate these possibilities, we examine three small, well-sampled regions with more consistent surface characteristics during light and dark seasons. These regions are shown in Figure 9. The first is a small box including and immediately surrounding the islands of Franz Josef Land, 80 - 82˚ N, 45 - 65˚ E. This region contains three surface stations and has a consistent record from 1971 through 2007, excluding only 2002-2004. Franz Josef Land was chosen due to its nearly perpetually ice-

bound state, so satellite observations can be compared to one another and surface observations over an icy surface during light and dark seasons. An oceanic region that is ice-free in all seasons (Ocean Box) was chosen in the Atlantic west of Norway, 60 - 70˚ N, 0 - 20˚ E Within this box, all satellite and surface observations over land have been excluded so only measurements over water are compared. During winter the Gulf of Bothnia, which is on the eastern side of this box, is covered in ice, so wintertime observations are excluded past 18˚ E. Finally, a box with 100% land cover was chosen (60 - 70˚ N, 80 - 100˚ E).

Figure 15 shows annual cycles of long-term averaged monthly total cloud cover for each sub-region in this study. Over open water, the TOVS shows greater cloud cover year-round by 5 - 10%, as well as a less exaggerated annual cycle. The APP-x cycle appears to closely match surface observations during sunlit months, but resembles the TOVS during darker months. In the case of observations over land, TOVS is once again showing greater cloud cover, especially during winter months, while the APP-x and surface observations show a nearly identical cycle. All three agree well between May and September. The yearly cycles shown over Franz Josef Land display a distinct 'high arctic' pattern with a summer maximum in cloud cover and a wintertime minimum. As was the case over open water, surface observations show less cloud cover during the dark time of the year when compared to satellite data. APP-x shows the

greatest cloud cover, especially during winter when APP-x cloud amounts are nearly 10% greater than the TOVS, which in turn are nearly 10% greater than the surface observations.

Time series of percent total cloud cover during each season for all three datasets over the three regions are shown in Figures 16 - 18. Seasonal average cloud cover, trends, and correlations for the time series in the figures are all compared in Tables 7 - 9.

Over the ocean region in Figure 16, higher cloud amounts are present in the TOVS data throughout the year and surface observations show cloud amounts similar to the APP-x except during winter. As was shown during the annual cycles, surface observations record 5 - 10% less cloud cover when compared with satellite observations. Interannual variability over the ocean is generally lower than over ice or the land region, and trends for the period of overlap all agree in sign for the ocean box. Trends in the ocean box also show the lowest magnitude, < 1% / decade. Correlations among the three time series are positive over the ocean, especially during spring and summer. Surface observations tend to correlate best with the APP-x cloud cover time series.

Land total cloud cover time series are compared in Figure 17. Once again, higher cloud amounts are seen in the TOVS data throughout the year, while APP-x cloud amounts and surface observed amounts agree more closely. Trends for the TOVS data and surface observations agree in sign during every

season, but disagree with the APP-x trends in spring and autumn. Uncertainty of the trends is similar for all three sources throughout the year. The time series all correlate positively with each other and the correlation coefficients are greater during spring and summer when the Arctic is mostly illuminated by sunlight. TOVS and surface data correlate most strongly except during winter.

Time series of cloud cover detected over the icy surface on and surrounding Franz Josef Land are shown in Figure 18. Amounts agree well between data sources during spring and autumn, but during winter APP-x data shows a higher cloud amount, and during summer TOVS shows a lower amount. Wintertime trends agree between the TOVS and APP-x, but surface observations show an increase where the satellites are showing a very substantial decrease in cloud cover. Interannual variability is also large in all three during wintertime, but more so in the satellite data than in the surface data. All three data sets show clouds strongly increasing during spring and less substantial trends during summer, with surface observations agreeing with the TOVS in summer, and disagreeing with both TOVS and APP-x during autumn. IAV is the highest of all regions over Franz Josef Land; this is no doubt partially due to the limited areal extent of the defined region. Surface observations and satellite data correlate marginally well during spring and summer, but are uncorrelated during autumn and winter. The correlations between TOVS and APP-x data are similar to those for the other regions.

To summarize, our initial comparisons of surface-observed cloud cover with satellite observations over the entire Arctic showed poor agreement. However, more consistency is seen when a comparison is made in smaller regions, especially in the correlation of interannual variations of the time series. Trends in cloud amounts from differing sources still show conflict over land and especially over ice. Correlations between surface and satellite observations also suffer most an icy surface during polar night. This poor correlation over ice during winter could be due to individual observers not detecting thin, very cold clouds in a dark environment, though this was not a problem over other surfaces. In fact, surface observations passing illuminance criteria over ice should have better light than the equivalent over bare land or ocean since the white surface can reflect incident moonlight, further illuminating a cloud deck. Satellite cloud detection during the Arctic winter could be problematic due to the limited number of channels available without any visible radiation, or with large, persistent inversions causing difficulty properly assessing the temperature of different layers within the atmosphere. Satellite datasets that were analyzed in this work have shown a curious tendency, with cloud amounts from many geographically different regions showing nearly identical interannual variations in all Arctic grid boxes during winter (Figure 19). Such a tendency was not observed when comparing time series of surface observations in different grid boxes. This suggests that satellite cloud detection during winter may be

affected by changes in instrumentation. This analysis suggests that there is agreement between satellite and surface based cloud datasets when compared over small, well sampled regions in spring and summer, but interannual variations found in cloud datasets over the Arctic are questionable, particularly during the Arctic winter, and that further study and processing of observations is still necessary.

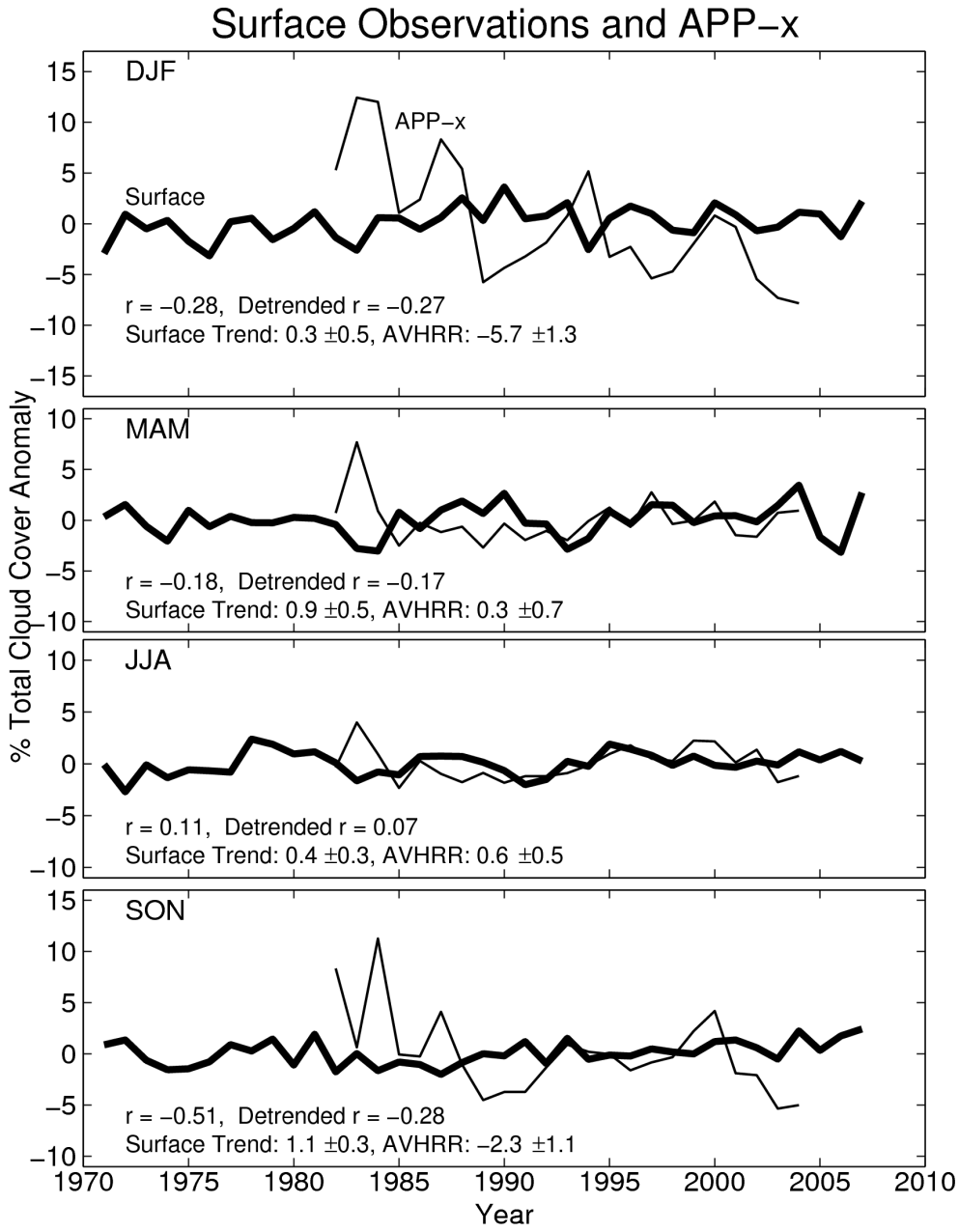

Figure 13, Surface Observations and APP-x. Anomaly time series of surface observed Arctic total cloud cover and that observed by the AVHRR Polar Pathfinder extended (APP-x) for 60˚ - 90˚ N.

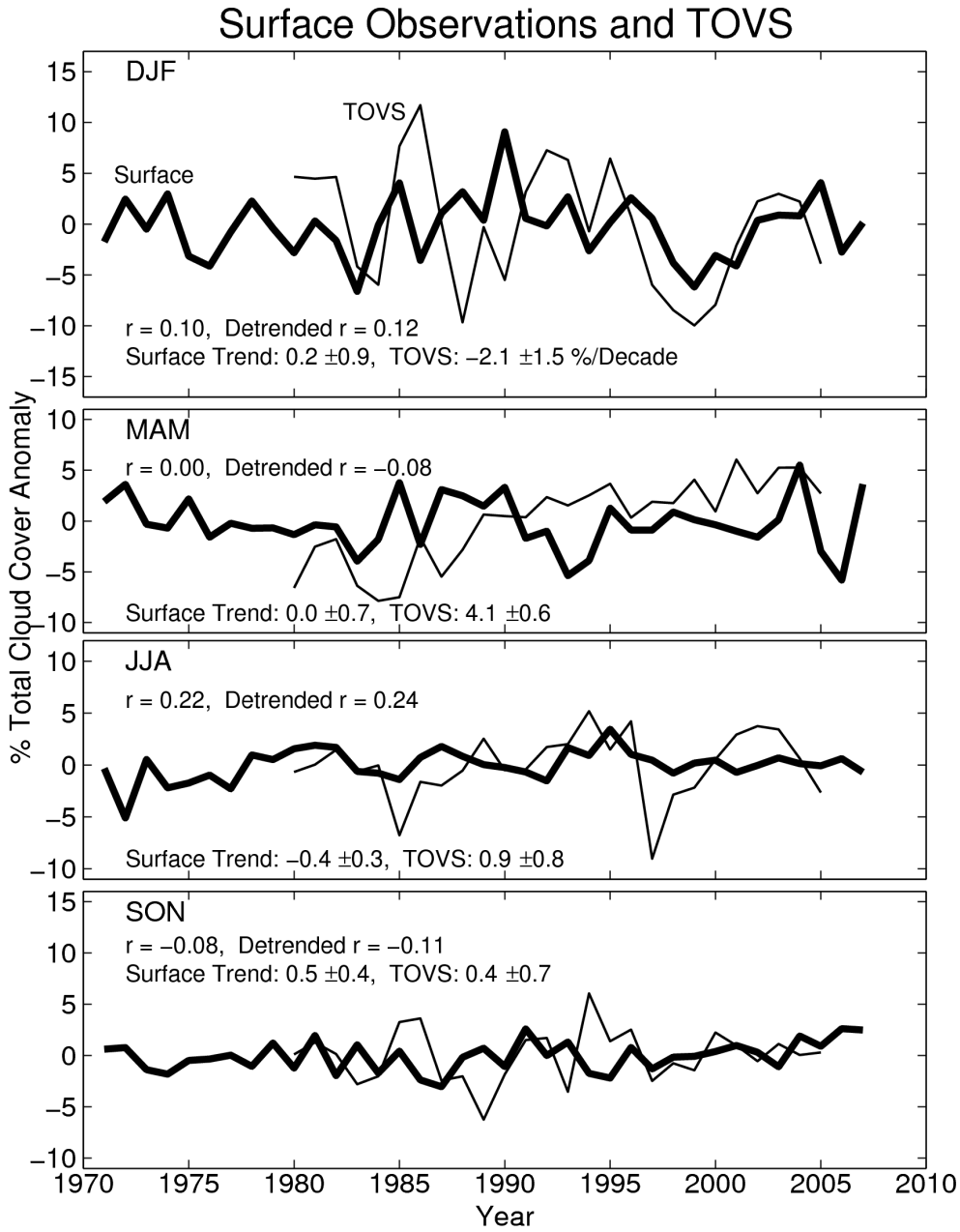

Figure 14, Surface Observations and TOVS. Anomaly time series of surface observed total cloud cover and that observed by the TOVS polar pathfinder over Arctic ocean areas, 60˚ - 90˚ N.

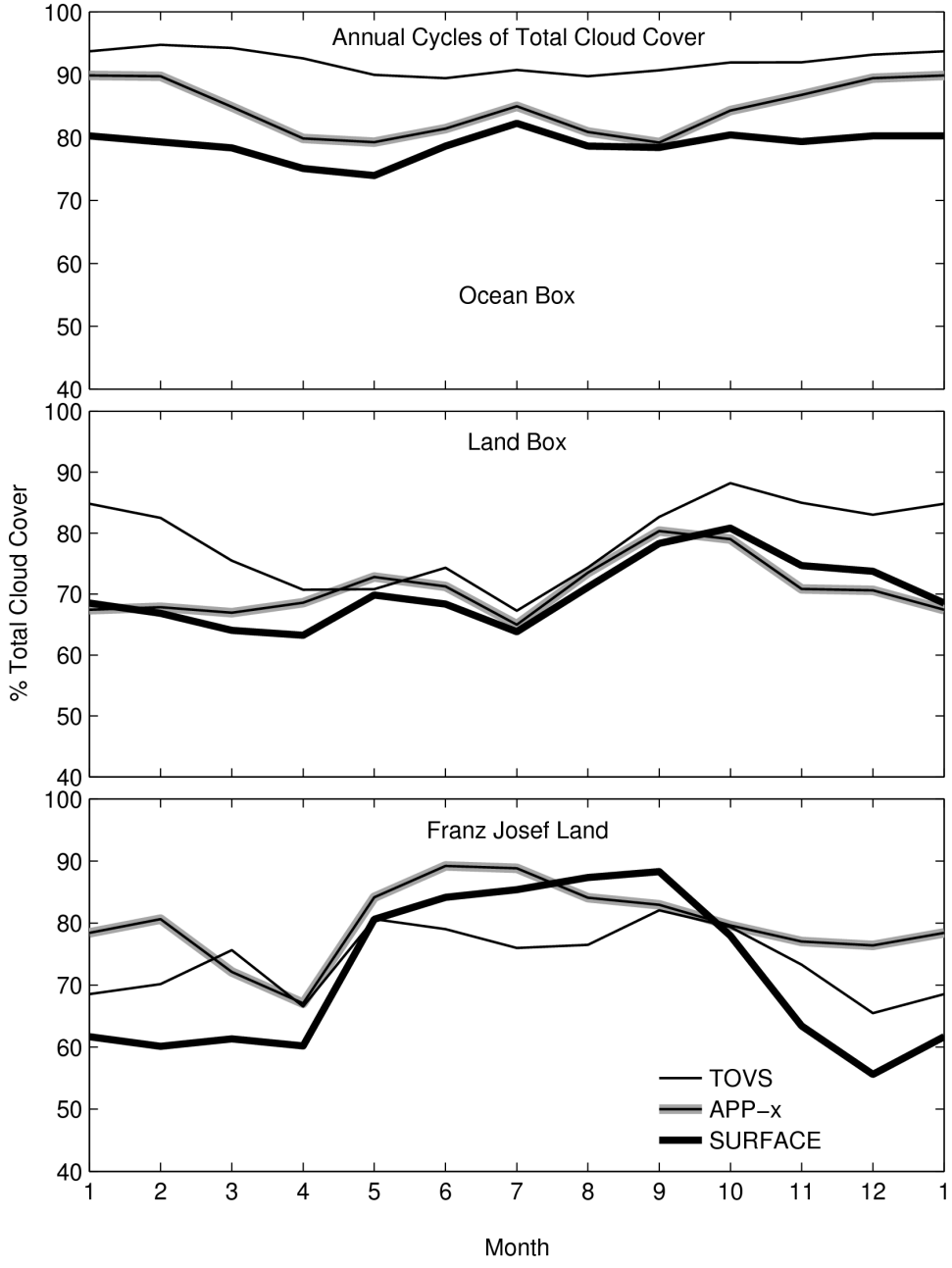

Figure 15, Annual Cycles of Cloud Cover. Annual cycles of total cloud cover over open ocean (top), land (middle) and ice (bottom) as detected by TOVS, APP-x and surface observations. The three boxes are defined in Figure 9.

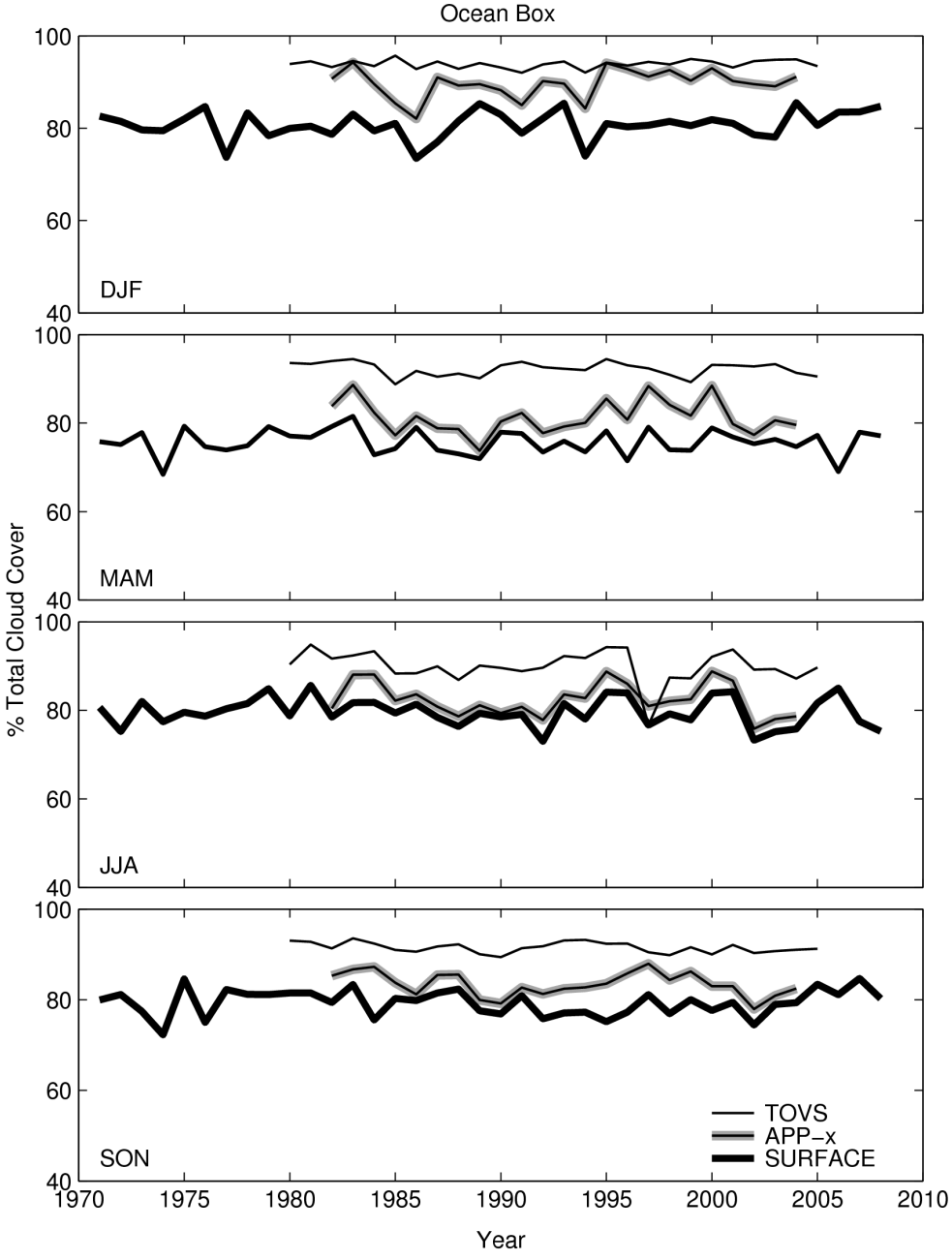

Figure 16, Time Series of Cloud Cover over Ocean. Time series of total cloud cover during all four seasons as reported by TOVS, APP-x and surface observations over an open ocean surface.

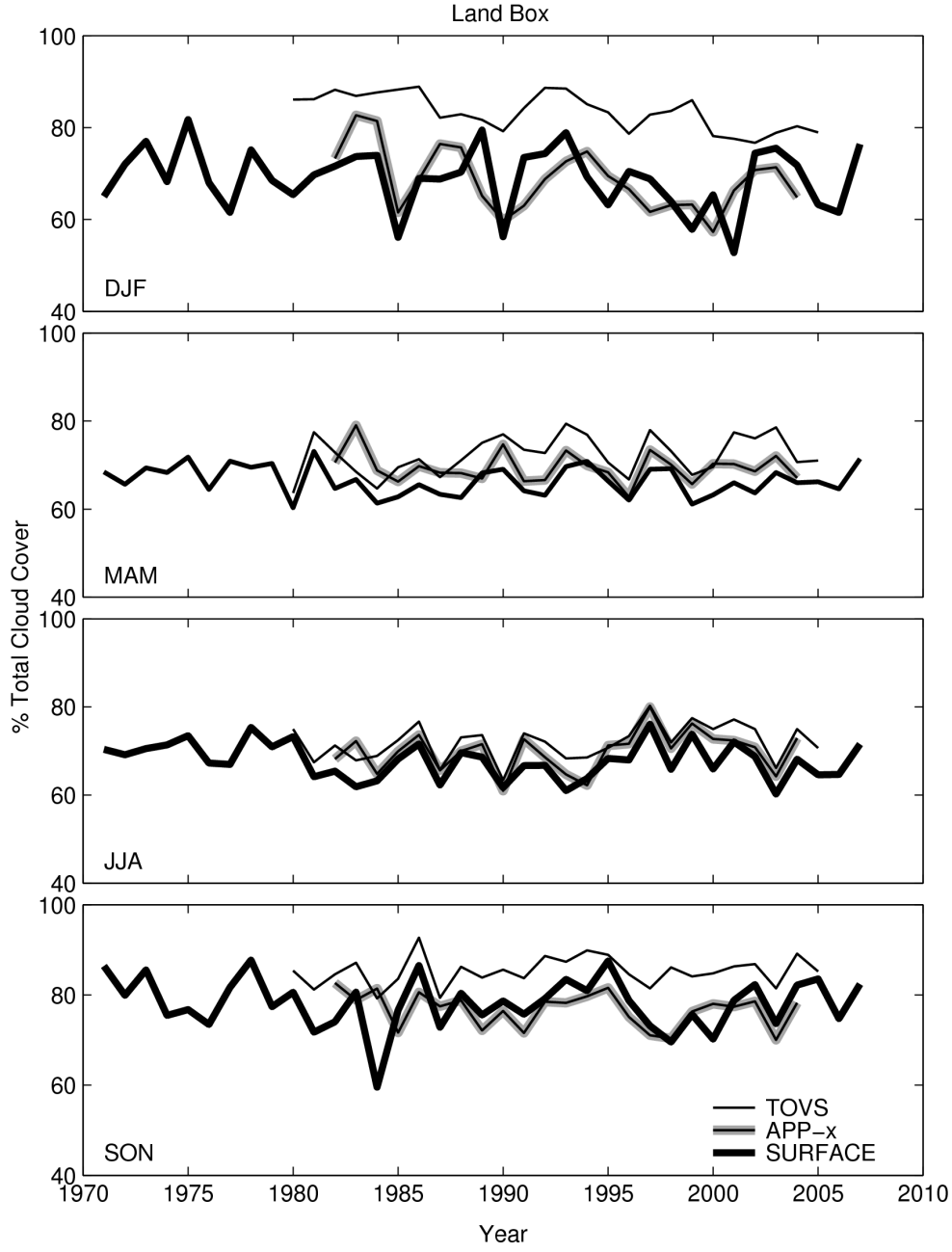

Figure 17, Time Series of Cloud Cover over Land. Time series of total cloud cover during all four seasons as reported by TOVS, APP-x and surface observations over a land surface.

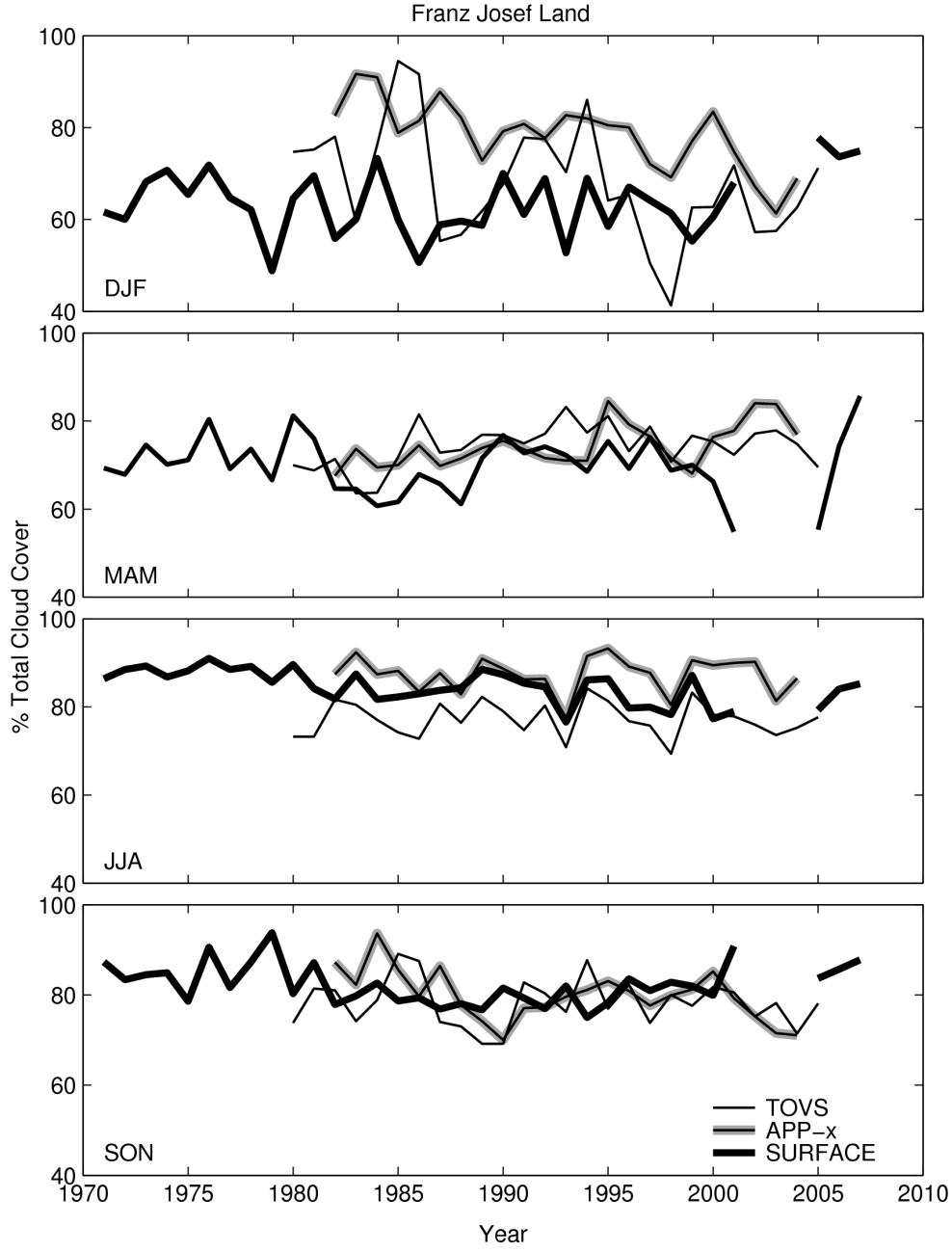

Figure 18, Time Series of Cloud Cover over Ice. Time series of total cloud cover during all four seasons as reported by TOVS, APP-x and surface observations over an ice surface.

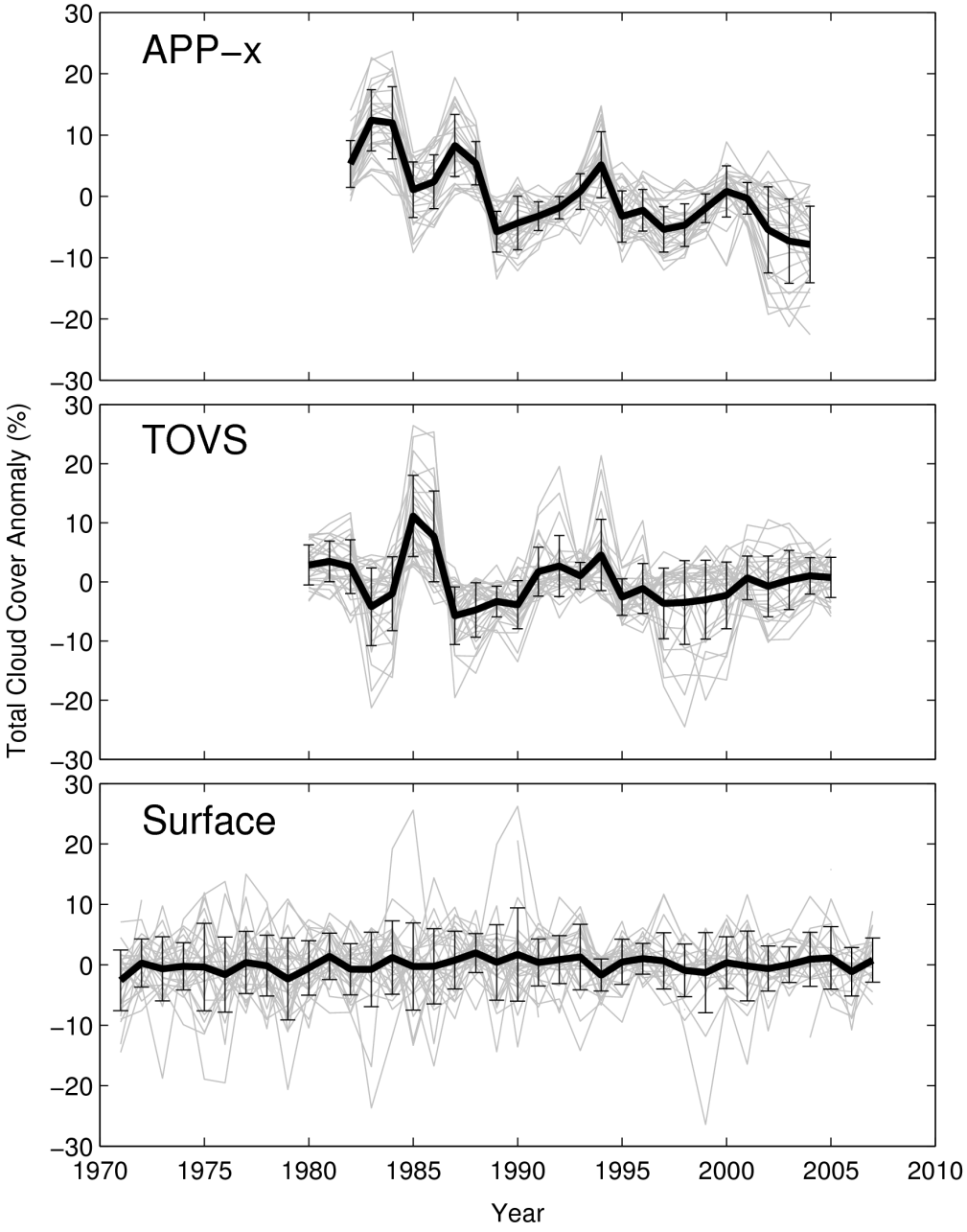

Figure 19, Timeseries of Cloud Data from Satellites and Surface Observations during Winter. Surface and satellite observed time series of wintertime (DJF) total cloud cover anomaly for individual 10 x 10-degree grid boxes (gray lines), the Arctic average (black line) and error bars showing the standard deviation of seasonal means.

Table 7, Cloud Amounts in Sub-Regions. Comparison of average cloud amounts (percent) in three grid-boxes determined from surface observations and from two satellite instruments: TIROS Operational Vertical Sounder (TOVS, Francis & Schweiger 1999, 2008) and AVHRR Polar Pathfinder (APPx, Wang & Key 2005).

a) Franz Josef Land (Ice Surface)

	SURF	TOVS	APPx
DJF	64	68	78
MAM	70	74	74
JJA	85	77	87
SON	82	78	80
Annual	75	74	80

b) Land Box (Land Surface)

	SURF	TOVS	APPx
DJF	69	83	69
MAM	67	72	69
JJA	68	72	70
SON	78	85	77
Annual	71	78	71

c) Ocean Box (Liquid Water Surface)

	SURF	TOVS	APPx
DJF	81	94	90
MAM	76	92	81
JJA	80	90	82
SON	79	92	83
Annual	79	92	84

Table 8, Correlations Among Cloud Data over Sub-Regions. Correlation of IAVs of total cloud cover inferred from different data sources: Surface observations (SURF), AVHRR Polar Pathfinder (APPx), and TIROS Operational Vertical Sounder (TOVS). The value given is the correlation coefficient multiplied by 100. Time spans: APPx & SURF 1982-2004, TOVS & SURF 1980-2005, APPx & TOVS 1982-2004.

a) Franz Josef Land (Ice Surface)

	APPx & SURF	TOVS & SURF	TOVS & APPx
DJF	1	6	35
MAM	28	41	34
JJA	55	46	78
SON	-3	3	44
Mean	20	24	48

b) Land Box (Land Surface)

	APPx & SURF	TOVS & SURF	TOVS & APPx
DJF	47	18	35
MAM	59	78	39
JJA	83	91	88
SON	27	78	41
Mean	54	66	51

c) Ocean Box (Liquid Water Surface)

	APPx & SURF	TOVS & SURF	TOVS & APPx
DJF	54	43	43
MAM	70	54	52
JJA	92	59	52
SON	48	23	45
Mean	66	45	48

Table 9, Trends of Cloud Data over Sub-Regions. Seasonal average trends (percent per decade) from 1982-2004 of total cloud cover obtained from three data sources: Surface observations (SURF), AVHRR Polar Pathfinder (APPx), and TIROS Operational Vertical Sounder (TOVS).

a) Franz Josef Land (Ice Surface)

	SURF	TOVS	APPx
DJF	1.5 ± 2.3	-7.0 ± 3.3	-8.8 ± 1.6
MAM	3.3 ± 2.2	2.9 ± 1.3	4.2 ± 1.2
JJA	-1.8 ± 1.3	-1.0 ± 1.1	0.2 ± 1.2
SON	2.1 ± 1.2	-1.2 ± 1.6	-4.3 ± 1.5
Annual	1.3 ± 1.7	-1.6 ± 1.8	-2.2 ± 1.4

b) Land Box (Land Surface)

	SURF	TOVS	APPx
DJF	-1.4 ± 2.3	-3.7 ± 0.9	-4.7 ± 1.8
MAM	0.8 ± 0.9	1.7 ± 1.2	-0.4 ± 1.1
JJA	1.4 ± 1.2	2.8 ± 1.1	1.6 ± 1.4
SON	0.7 ± 1.9	1.0 ± 1.0	-1.5 ± 1.2
Annual	0.4 ± 1.6	0.5 ± 1.0	-1.2 ± 1.4

c) Ocean (Liquid Water Surface)

	SURF	TOVS	APPx
DJF	0.2 ± 0.9	0.3 ± 0.3	0.6 ± 0.9
MAM	-0.1 ± 0.8	-0.2 ± 0.5	-0.1 ± 1.2
JJA	-0.5 ± 0.9	-0.8 ± 1.1	-0.8 ± 1.2
SON	-0.4 ± 0.7	-0.6 ± 0.3	-1.2 ± 0.8
Annual	-0.2 ± 0.8	-0.3 ± 0.5	-0.4 ± 1.0

7. CONCLUSIONS

The Arctic is shown to be a very cloudy region with an average of around 70 % cloud cover. Clouds are more prevalent over oceanic regions of the Arctic. A pronounced yearly cycle of cloud cover exists over the 'High Arctic'. Cloud cover displaying the High Arctic cycle is bimodal, with cloud cover high in summer and low in winter. Low stratiform clouds are responsible for this cycle, which has been attributed to the cloud response to the annual cycle in air temperature. This pattern is not entirely latitude-dependent, but instead appears to be geographically based upon the location of sea ice and the colder, continental regions within the Arctic.

Significant trends are present in Arctic cloudiness over the ocean and land. The trends are not uniform over the Arctic, but large regions displaying similar trends are common. Arctic clouds are changing differently over the land and ocean, but overall the trend from 1971 through 2007 shows a slight increase in total cloud cover during all seasons. Low clouds appear most responsible for this trend, partially offset by decreases in precipitating cloud amounts. This decrease in precipitating clouds has not been forecast or simulated in existing modeling studies. Combined, these cloud changes are likely to enhance warming in the Arctic during much of the year.

Clouds over sea ice show an association with warming temperatures and

decreasing sea ice except during summer. As observed over the entire Arctic, there is a substantial decreasing trend in precipitating clouds, but an even larger increase in low, stratiform cloud cover. A possible cause for this could be changing aerosols within the Arctic atmosphere, though trends in current aerosol data suggest otherwise. During autumn, a strong, positive low-cloud response to reduced sea ice is seen. Overall, relationships between ice, temperature and clouds indicate that cloud trends may enhance the warming of the Arctic and may be acting to accelerate the decline of Arctic sea ice.

Interannual variations and trends obtained from satellite observations disagree with those obtained from surface observations, when compared for the entire Arctic, especially in the dark seasons (autumn and winter). Better agreement is seen over small geographic regions except during winter over an icy surface. The exact cause for this disagreement remains unknown, but winter/nighttime detection issues or sparse and inadequate surface observations could be to blame. Wintertime interannual variations in satellite data from different geographical regions have shown a peculiar tendency to oscillate in phase, which may indicate sensor problems during the polar night. Further study of all of these datasets is necessary to attempt to improve their accuracies for studies of interannual variations and trends.

REFERENCES

Beesley, J. A. 2000: Estimating the effect of clouds on the arctic surface energy budget. *J. Geophys. Res.* 105(D8), 10,103-10,117.

Beesley, J. A., and R. E. Moritz, 1999: Toward an explanation of the annual cycle of cloudiness over the Arctic Ocean. *J Climate*. **12**, 395-415.

Brodzik, M. J., and K. W. Knowles, 2002: EASE-grid: A versatile set of equal-area projections and grids. In M. Goodchild (Ed.) *Discrete Global Grids*. Santa Barbara, California USA: National Center for Geographic Information & Analysis

Curry, J.A., and G.F. Herman, 1985: Relationships between large-scale heat and moisture budgets and the occurrence of Arctic stratus clouds. *Mon. Wea. Rev*., 113, 1441-1457.

Curry, J. A., and E. E. Ebert, 1992: Annual cycle of radiation fluxes over the Arctic Ocean: Sensitivity to cloud optical properties. *J. Climate*, **5**, 1267-1280.

Francis, J. A., and A. J. Schweiger, 1999, updated 2008: TOVS pathfinder path-P daily and monthly polar gridded atmospheric parameters. National Snow and Ice Data Center (NSIDC), Boulder, Colorado http://nsidc.org/data/nsidc-0027.html

Francis, J. A., and E. Hunter, 2006: New insight into the disappearing arctic seaice, *Eos, Trans. Amer. Geophys. Union*. Vol 87, No. 46, 509-524.

Garrett, T. J., and C. Zhao, 2006: Increased Arctic cloud longwave emissivity associated with pollution from mid-latitudes. *Nature*, 440, 10.1038/nature04636, 787-789.

Gorodetskaya, I. V., and L. B. Tremblay, 2008: Arctic cloud properties and radiative from observations and their role in sea ice decline predicted by the NCAR CCSM3 model during the 21st century, In: *Arctic Sea Ice Decline:*

Observations, Projections, Mechanisms, and Implications, [Eds. E. DeWeaver, C. M. Bitz, and L.-B. Tremblay]. *Geophys Monogr Ser*, AGU, Washington, vol 180, pp 213–268

Hahn, C.J., and S.G. Warren, 1999 (Updated 2009): *Extended Edited Cloud Reports from Ships and Land Stations over the Globe, 1952-1996*. Numerical Data Package NDP-026C, Carbon Dioxide Information Analysis Center (CDIAC), Department of Energy, Oak Ridge, Tennessee (Documentation, 79 pages).

Hahn, C.J., and S.G. Warren, 2003: *Cloud Climatology for Land Stations Worldwide, 1971-1996*. Report NDP-026D, 35 pp. Carbon Dioxide Information Analysis Center, Oak Ridge, Tennessee, USA. http://cdiac.ornl.gov/ftp/ndp026d/

Hahn, C.J., and S.G. Warren, 2007 updated 2009: *Cloud Climatology for Ship Observations Worldwide, 1954-2008*. Report NDP-026E, Carbon Dioxide Information Analysis Center, Oak Ridge, Tennessee, USA. http://cdiac.ornl.gov/ftp/ndp026e/

Hahn, C.J., S.G. Warren, and J. London, 1995: The effect of moonlight on observation of cloud cover at night, and application to cloud climatology. *J. Climate,* **8**, 1429-1446.

Herman, G., and R. Goody, 1976: Formation and persistence of summertime Arctic stratus clouds. *J. Atmos. Sci*, **33**, 1537-1553.

Intrieri, J.M., C.W. Fairall, M. D. Shupe, P. O. G. Persson, E. L. Andreas, P. S. Guest, and R. E. Moritz, 2002: An annual cycle of Arctic surface cloud at SHEBA. *J. Geophys. Res.* 107(C10), 8039, doi:10.1029/2000JC000439.

Kalnay, E., M. Kanamitsu, R. Kistler, W. Collins, D. Deaven, L. Gandin, M. Iredell, S. Saha, G. White, J. Woollen, Y. Zhu, M. Chelliah, W. Ebisuzaki, W. Higgins, J. Janowiak, K. C. Mo, C. Ropelewski, J. Wang, A. Leetmaa, R. Reynolds, R. Jenne, and D. Joseph, 1996: The NCEP/NCAR 40-year reanalysis project, *Bull. Amer. Meteor. Soc.*, 77, 437-470.

Knowles, K., 2004: EASE-Grid land cover data resampled from AVHRR Global 1

km land cover, Version 2, March 1992 - April 1993. Boulder CO, USA: National Snow and Ice Data Center. Digital Media.

Kay, J. E., T. L'Ecuyer, A. Gettelman, G. Stephens, and C. O'Dell, 2008: The contribution of cloud and radiation anomalies to the 2007 Arctic sea ice extent minimum. *Geophys. Res. Lett.* 35, L08503, doi:10.1029/2008GL033451.

Lanzante, J.R., 1996: Resistant, robust and non-parametric techniques for the analysis of climate data: Theory and examples, including applications to historical radiosonde station data. *Int. J. Climatol*,. 16, 1197-1226.

NSIDC, 2008: http://nsidc.org/news/press/20081002_seaice_pressrelease.html

Quinn, P.K., G. Shaw, E. Andrews, E.G. Dutton, T. Ruoho-Airola, and S.L. Gong, 2007: Arctic haze: current trends and knowledge gaps, *Tellus B,* **59**, pp. 99–114.

Rigor, I., R. Colony, and S. Martin, 2000: Variations in surface air temperature observations in the Arctic, 1979 - 1997, *J. Climate*, 13(5), 896-914.

Rigor, I. G., J.M. Wallace, and R. L. Colony, 2002: On the response of sea ice to the Arctic Oscillation, *J. Climate*, 15(18), 2546–2663.

Schweiger, A. J., 2004: Changes in seasonal cloud cover over the Arctic seas from satellite and surface observations, *Geophys. Res. Lett*., 31, L12207, doi:10.1029/2004GL020067.

Schweiger, A. J., R. W. Lindsay, S. Vavrus, and J. A. Francis, 2008: Relationships between Arctic sea ice and clouds during autumn, *J. Climate*, 21, 4799-4810.

Shupe, M. D., and J. M. Intrieri, 2004: Cloud radiative of the Arctic surface: The influence of cloud properties, surface albedo, and solar zenith angle, *J. Climate*, 17, 616-628.

Stroeve, J., M. Serreze, S. Drobot, S. Gearheard, M. Holland, J. Maslanik, W.

Meier, and T. Scambos, 2008: Arctic sea ice extent plummets in 2007, *Eos Trans. AGU*, 89(2), doi:10.1029/2008EO020001.

Thompson, D.W.J., and J.M. Wallace, 1998: The Arctic Oscillation signature in the wintertime geopotential height and temperature fields, *Geophys. Res. Lett.*, 25, 9, 1297-1300.

Vavrus, S., 2004: The impact of cloud feedbacks on Arctic climate under greenhouse , *J. Climate*, 17, 603-615.

Vavrus, S., M. Holland., and D. Bailey, 2008a: The role of Arctic clouds during intervals of rapid sea ice loss, *Eos Trans. AGU*, 89(53), Fall Meet. Suppl., Abstract C51A-0539.

Vavrus, S., D. Waliser, A. Schweiger, and J. Francis, 2008b: Simulations of 20th and 21st century Arctic cloud amount in the global climate models assessed in the IPCC AR4. *Climate Dynamics,* , doi:10.1007/s00382-008-0475-6.

Vowinckel, E., 1962: Cloud amount and type over the Arctic. *Publications in Meteorology*, No. 51. Arctic Meteorology Research Group, McGill University, Montreal. 63 pp.

Vowinckel, E., and S. Orvig, 1970: The climate of the North Polar Basin. *World Survey of Climatology,* Vol. 14, *Climates of the Polar Regions,* S. Orvig, Ed., Elsevier, 129–252.

Walsh, J. E., V. Kattsov, D. Portis, and V. Meleshko, 1998: Arctic precipitation and evaporation: model results and observational estimates. *J. Climate,* 11, 72-87.

Walsh, J. E., and W. L. Chapman, 1998: Arctic cloud-radiation-temperature associations in observational data and atmospheric reanalyses, *J. Climate*, 11, 3030-3045.

Walsh, J. E., V. M. Kattsov, W. L. Chapman, V. Govorkova, and T. Pavlova, 2002: Comparison of Arctic climate simulations by uncoupled and coupled global models. *J. Climate*, 15, 1429-1446.

Wang, X., and J. R. Key, 2005: Arctic surface, cloud and radiation properties based on the AVHRR polar pathfinder dataset. Part II: Recent trends, *J. Climate*, 18, 2575-2593.

Warren, S. G., and C.J. Hahn, 2002: Cloud climatology. *Encyclopedia of Atmospheric Sciences,* 476-483. Oxford University Press.

Warren, S.G., R. M. Eastman and C.J. Hahn, 2007: A survey of changes in cloud cover and cloud types over land from surface observations, 1971-1996. *J. Climate*, 20, 717-738.

Warren, S. G., I. G. Rigor, N. Untersteiner, V. F. Radionov, N. N. Bryazgin, Y. I. Aleksandrov, and R. Colony, 1999: Snow depth on arctic sea ice, *J. Climate,* 12, 1814-1829.

WMO, 1974: *Manual on Codes*. Vol. 1. World Meteorological Organization Publication 306, 348 pp.

Woodruff, S.D., R.J. Slutz, R.L. Jenne, and P.M. Steurer, 1987: A comprehensive ocean-atmosphere data set. *Bull. Amer. Meteor. Soc.*, 68, 1239-1250.

Woodruff, S.D., H.F. Diaz, J.D. Elms, and S.J. Worley, 1998: COADS Release 2 data and metadata enhancements for improvements of marine surface flux fields. *Phys. Chem. Earth*, 23.

Worley, S.J., S.D. Woodruff, R.W. Reynolds, S.J. Lubker, and N. Lott, 2005: ICOADS Release 2.1 data and products. *Int. J. Climatol.*, **25**, 823-842.